

See discussions, stats, and author profiles for this publication at: <https://www.researchgate.net/publication/231399106>

The Electrode/Electrolyte Interface – A Status Report

ARTICLE *in* THE JOURNAL OF PHYSICAL CHEMISTRY · JULY 1993

Impact Factor: 2.78 · DOI: 10.1021/j100130a007

CITATIONS

153

READS

16

9 AUTHORS, INCLUDING:



Kingo Itaya

Tohoku University

246 PUBLICATIONS 8,446 CITATIONS

SEE PROFILE

FEATURE ARTICLE

The Electrode/Electrolyte Interface—A Status Report

Allen J. Bard*

Department of Chemistry and Biochemistry, The University of Texas at Austin, Austin, Texas 78712

Hector D. Abruña

Department of Chemistry, Baker Laboratory, Cornell University, Ithaca, New York 14853

Chris E. Chidsey

Department of Chemistry, Stanford University, Stanford, California 94305

Larry R. Faulkner

Department of Chemistry, University of Illinois at Urbana-Champaign, Urbana, Illinois 61801

Stephen W. Feldberg

Department of Applied Science, Brookhaven National Laboratories, Brookhaven, Upton, Long Island, New York 11973

Kingo Itaya

Department of Chemical Engineering, Faculty of Engineering, Tohoku University, Sendai 980, Japan

Marcin Majda

Department of Chemistry, University of California at Berkeley, Berkeley, California 94720

Owen Melroy

IBM Almaden Research Center, 650 Harry Road, San Jose, California 95120-6099

Royce W. Murray

Department of Chemistry, Venable and Kenan Laboratories, University of North Carolina, Chapel Hill, North Carolina 27599

Marc D. Porter

Department of Chemistry, Iowa State University, Ames, Iowa 50011

Manuel P. Soriaga

Department of Chemistry, Texas A&M University, College Station, Texas 77843

Henry S. White

Department of Chemistry, University of Utah, Salt Lake City, Utah 84112

Received: March 9, 1993

This is a report of a workshop on the “state of the art” and potential future directions in the study of the electrode/electrolyte interface. Recent advances in experimental capabilities of characterizing the structure of the interface, e.g., through the use of such techniques as scanning tunneling microscopy and X-ray methods, are described. New approaches to studies of interfacial dynamics and materials aspects of the electrode/electrolyte interface are also discussed.

Contents

I. Introduction	7148
II. Structural characterization of the electrode/electrolyte interface	7149
A. Electrode characterization	7149
1. <i>In-situ</i> techniques	7149
a. Scanning probe microscopies	7150
b. Ultramicroelectrodes and scanning electrochemical microscopy	7152
c. X-ray methods	7153
d. Nonlinear optical methods	7156
2. UHV (<i>ex-situ</i>) electrochemical techniques	7156
B. Electrolyte characterization	7158
1. Experimental measurements	7158
2. Theory and simulations	7158
III. Interfacial dynamics	7159
A. Mechanisms and elementary processes	7159
B. Experimental characterization of heterogeneous electron-transfer rates	7159
1. Microelectrode techniques	7159
2. Surface-attached monolayers	7160
3. Open-circuit optical perturbations and pump-probe methods	7161
C. Interfacial movement of electrons and ions	7161
1. Electron transfer in the presence of interfacial charge	7161
2. Coupling of electron transfer and ion dynamics	7162
3. Intermolecular electron transfer at structured interfaces	7162
D. Catalysis	7162
E. Structural dynamics of electrode surfaces	7163
IV. Chemical materials and microstructures	7163
A. Introduction	7163
B. Electrodes with atomically definable interfaces	7163
C. Molecularly defined electrode surfaces and novel electrolyte media	7164
1. Coherently organized molecular structure at electrodes	7164
a. Self-assembled monomolecular films	7164
b. Selectivity in electrode reactions	7166
2. Environmental dynamics	7168
a. Solvent dynamics	7168
b. Dynamics of donor/acceptor sites within polymer films on electrodes	7168
c. Temperature	7169
V. Conclusions	7169

I. Introduction

Many important and interesting processes occur at interfaces; we discuss here the electrode/electrolyte interface. The corrosion of metals, the operation of electroanalytical sensors, the charging and discharging of batteries, the etching of semiconductors, and the electroplating of metals are all examples of processes that occur at this interface. Scientists have long studied electrochemical interfaces, partly because they are very important to technologies for generating and storing electrical energy and for synthesizing chemicals and materials. However, these are very

complex systems and experimentally difficult to study. They typically involve simultaneous consideration of poorly understood aspects of solid-state physics (interfacial atomic and electronic structure), of the liquid state (local structure and dynamics, especially as altered by an interface), and of patterns of chemical reactivity (processes involving species bound to surfaces). This lack of understanding has contributed to an inadequate experimental control over interfacial structure and reactivity, which has itself limited the development of improved understanding. It is not yet possible to address most issues in the field of the electrode/electrolyte interface with the precision that has existed for studies of bulk solids, of gas-phase chemistry, or even for molecules reacting in homogeneous liquids.

Electrochemical techniques have long been used to study such interfaces. While these methods remain valuable in elucidating the nature of such interfaces and the reactions that occur in their vicinity, they are largely based on macroscopic models which do not provide direct information about the interfacial structure. A large number of spectroscopic techniques, such as infrared and Raman spectroscopy, have also been used to probe the nature and orientation of species at electrode surfaces, but structural information at the atomic and molecular level remained elusive. However, recent advances in interfacial physics, in the chemistry and physics of liquids, and in electrochemistry have changed the picture. Several techniques have emerged that allow examination of interfaces with atomic resolution, such as *in-situ* X-ray methods and scanning probe microscopies. This has led to remarkable advances in our understanding of the structure of these interfaces. At the same time, interesting new structures, such as organized monolayer and polymer films, have been prepared on electrode surfaces, and the time window for electrochemical measurements has been extended down to the nanosecond regime. These have contributed to a new understanding of dynamic processes, such as mass and electron transfer, at interfaces.

Thus, in the last few years, advances in experimental capabilities have allowed studies of electrode/electrolyte interfaces in which the role of structure in electrochemical behavior can be evaluated on the molecular and atomic scale. Now is an appropriate time to review recent progress in the field, assess the state of the art, and discuss possible future directions and advances. To this end, a panel convened at Tahoe City, California, Aug. 10–14, 1992, under the auspices of the Department of Energy, Council on Materials Science. This paper represents the results of the deliberations of this panel. We divide the discussion of these issues into three parts: structural characterization, dynamics, and materials.

Structural characterization precedes synthesis, since progress in the preparation of new structures can only proceed if one can determine the nature of the starting materials and products. Moreover, a knowledge of structure is essential to the understanding of energetics and reactivity at interfaces. Electrochemical systems are almost always constructed to do something, rather than to be something; thus, dynamics are at the heart of purpose. Progress in understanding, then, depends heavily on the ability to elucidate mechanisms. It is essential to comprehend both single steps, such as interfacial electron transfer, and complex mechanisms, such as those involved in catalysis. Improved spatial and temporal capabilities in investigation of interfaces are leading to exciting possibilities for obtaining structural information on a time-resolved basis.

Synthesis of new structures and materials often has been the immediate purpose of exercising control over the local environment, allowing interfacial behavior to be understood more effectively. However, work in this area should be viewed in the context of a comprehensive theme in contemporary chemistry and materials science, namely, the development of general strategies for producing supermolecular assemblies, in which

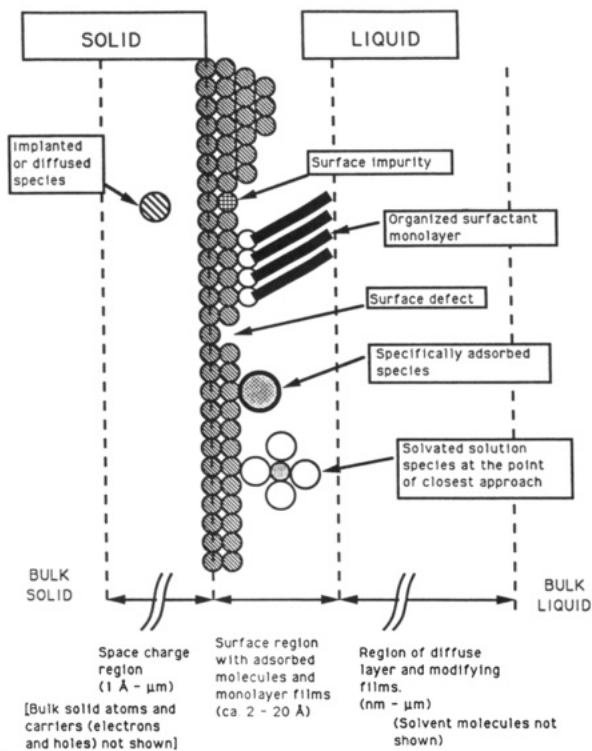


Figure 1. Schematic representation of the liquid–solid interfacial region showing possible species and features.³⁴⁶

assemblies of molecules effect a purpose (such as catalyzing a reaction, converting energy, or storing information) beyond the capability of a single molecule. Progress is being made along this line in many different venues. The electrode/electrolyte interface is among the most attractive, because it offers a platform for construction, as well as a convenient means of probing the structure and behavior and for coupling to macrosystems. Recent developments in synthesis at electrodes, especially through self-assembly, offer means for structural control of single reactive sites and for the precise placement of reactive centers with respect to each other and with respect to the electrode.

It is useful at the outset to describe the interfacial region as it pertains to the scope of this report. A schematic representation of the electrode/electrolyte interface is shown in Figure 1. While the actual *interface* (electrode surface) represents only the top layer of atoms on the electrode and the layer of adsorbed solvent and specifically adsorbed species, an *interfacial region* that is different from the bulk phases extends over considerably longer distances. Within the electrolyte this comprises the region of the diffuse layer as well as the region occupied by modifying overlayers (monolayers or thicker films). A space charge region also exists within the electrode. This is very narrow (at most a few angstroms) within metals but can be quite large with semiconductors, which have a lower density of carriers. A wide range of materials are used as electrodes and electrolytes. Electrode materials (electronic conductors) include noble metals (Pt, Au), active metals (Fe, Ni), carbon of various types, semiconductors (Si, CdS), electronically conductive polymers (polyaniline, polypyrrole), and organic conductors (TTF-TCNQ). Electrolyte phases (ionic conductors) include aqueous and nonaqueous solutions, ionically conductive polymers (polyethylene oxide, Nafion), and solid electrolytes (sodium β -alumina). Electrode surfaces can also be classified according to their structural definition (single crystal ("well-defined"), polycrystalline, amorphous) and also to the nature of any surface modification, e.g., by adsorbates, deposited atoms, organized or nonorganized monolayer films, polymer layers, or etching. Clearly, the range of materials involved in consideration of the electrode/electrolyte interface is enormous and cannot be uniformly covered in this report. We have thus

selected for discussion here a few examples of interfaces where recent advances in characterization have led to a new understanding of their properties. Many other important types of interfaces, such as those involved in corrosion or in semiconductor photoelectrochemistry, have been omitted. Similarly, a wide range of electrochemical and spectroscopic techniques have been employed to examine interfaces. Again, for brevity, we limit our discussion to some of the important advances that have been made during the last years that have set the stage for future developments. We attempt to point out the new capabilities and outstanding issues in three interrelated areas—structural characterization, dynamics, and materials aspects of electrode/electrolyte interfaces.

II. Structural Characterization of the Electrode/Electrolyte Interface

The past decade has spawned major advances in strategies and instrumentation for the characterization of the electrode/electrolyte interface. The empirical approaches have been conveniently classified as *ex-situ* or *in-situ*. The *ex-situ* methods are closely tied to ultra-high-vacuum (UHV) surface analytical techniques developed a decade earlier in the study of heterogeneous catalysis and microelectronics. In this scheme, the same UHV apparatus used for initial electrode surface preparation and characterization is employed later to study the same electrode surface after the electrochemical (EC) experiments; a variety of surface-sensitive analytical tools can be directly applied to assay the surface composition, geometric arrangement, and electronic structure after removal (emersion) of the electrode from solution.¹ The principal limitation in UHV-EC and other *ex-situ* techniques is the need to establish the relationship between the surface prior to and after emersion from solution into vacuum. By definition, *in-situ* techniques examine the electrode surface under electrochemical conditions. Hence, when possible, it is the approach of choice; *in-situ* methods, however, are not as numerous as *ex-situ* techniques. A requirement in all *in-situ* methods is the ability to distinguish between the response of species located at the electrode surface from that of the same analyte distributed in the solution phase. This demand often leads to restrictions in cell geometry and electrolyte concentration. Nevertheless, the evolution of *in-situ* methods is now greatly increasing our understanding of selected electrode/electrolyte interfacial processes.

A. Electrode Characterization. *1. In-Situ Techniques.* Progress in the development and exploitation of spectroelectrochemical techniques has proceeded at a rapid pace. The availability of synchrotron radiation and the emergence of scanning probe techniques such as scanning tunneling microscopy (STM) and atomic force microscopy (AFM) have provided the capability of interrogating the atomic structure of the electrode surface as well as that of adsorbed layers. The application of these techniques has allowed a very detailed picture of the static structure of well-defined surfaces and ordered adlayers. One of the important challenges for the next decade will be developing techniques to probe the dynamics of these structures.

Although much of the atomistic information has come from the X-ray-based techniques and scanned probe microscopy, the application of other spectroelectrochemical methods continues to provide important complementary information, such as the molecular orientation of adsorbates. Among the most important techniques are infrared reflection-absorption spectroscopy (IRAS) and surface-enhanced Raman spectroscopy (SERS). Since the pioneering work in 1980,² IRAS has experienced explosive growth, in part because it does not require the surface roughening procedures necessary in SERS and, hence, can be applied to study processes at single-crystal electrodes. IRAS has become a well-established *in-situ* characterization technique that has found application to a wide variety of problems, such as the identification of molecular adsorbates, the determination of their orientation, the study of the structure of self-assembled monolayers, char-

acterization of the double layer, and the identification of short-lived intermediates.³ While receiving less recent attention than IRAS, SERS has at least two important virtues: (i) many Raman-allowed transitions are IR-forbidden and (ii) low-frequency vibrations down to 5 cm^{-1} are accessible. SERS has been applied to studies ranging from the probing of molecular events to the orientation of molecules within the double layer.⁴ The necessity of roughening the surface to obtain the large enhancement in signal which SERS enjoys has rendered it inapplicable to well-defined single-crystal surfaces. However, progress has been made in employing normal Raman spectroscopy at smooth, albeit polycrystalline, electrodes.⁵

The availability of high magnetic fields and ultrafast digitizers has paved the way for the use of nuclear magnetic resonance (NMR) spectroscopy in the study of high-surface-area catalysts.⁶ Although the application of surface NMR as an *in-situ* technique for interfacial electrochemistry has long been anticipated, actual implementation is quite recent⁷ and is still fraught with difficulties. However, preliminary work on the mode of binding of ^{13}CO on polycrystalline, high-surface-area Pt has been reported.⁸ Additional research, such as magic-angle spinning NMR measurements with metal electrodes, is required for further progress in NMR-EC. Since NMR itself is not a highly sensitive technique, its use in electrochemical systems is limited to polycrystalline, high-area electrode surfaces. Nevertheless, the benefits of NMR spectroscopy, as evidenced by the major advances in solution and (bulk) solid-state chemistry, should justify further research in this area.

The radioactive labeling technique has been proposed as one of the more direct *in-situ* sources of information concerning adsorption at the electrode/electrolyte interface.⁹ This method is based upon a direct relationship between surface count rate and the interfacial concentration (Γ) of the labeled adsorbate; provided radioactive isotopes are available any type of surface-active material can be studied. Experimental measurements can focus on the kinetics and energetics of the adsorption process. Recent advances in this technique now permit investigations at well-defined, low-area, single-crystal electrode surfaces; specific interfacial systems studied have ranged from reversible or irreversible adsorption of ionic and molecular species to electrodeposition of ultrathin metal films.¹⁰

The electrochemical quartz crystal microbalance (EQCM) has also emerged as an important technique.¹¹ Unfortunately, its sensitivity to surface morphology and stress, as well as an incomplete understanding of the coupling between the motion of the quartz crystal and the liquid, can result in ambiguities in the interpretation of data. Nevertheless, the ability to provide such a fundamental measurement, that of mass, makes it exceptionally powerful.

(a) *Scanning Probe Microscopies. Scanning Tunneling and Atomic Force Microscopies.* Although classical electrochemical methods such as cyclic voltammetry have provided remarkable sensitivity for the characterization of submonolayer processes occurring at electrode/liquid interfaces, until recently there were few *in-situ* methods for the structural determination of the electrode surface at the atomic level. However, early studies showed that the scanning tunneling microscope (STM) can operate in electrolyte solutions;¹²⁻¹⁴ further studies have demonstrated that STM and a related technique, atomic force microscopy (AFM), can be used to characterize suitable solid/liquid interfaces with atomic resolution.^{15,16}

In electrolyte solutions, it is desirable to control the electrode potential of the substrate and the tip independently with respect to a reference electrode. The apparatus, called the electrochemical STM, allows *in-situ* observation of electrochemical reactions under potentiostatic conditions using a four-electrode configuration. Conditions are maintained so that mainly a tunneling current flows between the substrate and the tip, while a faradaic current

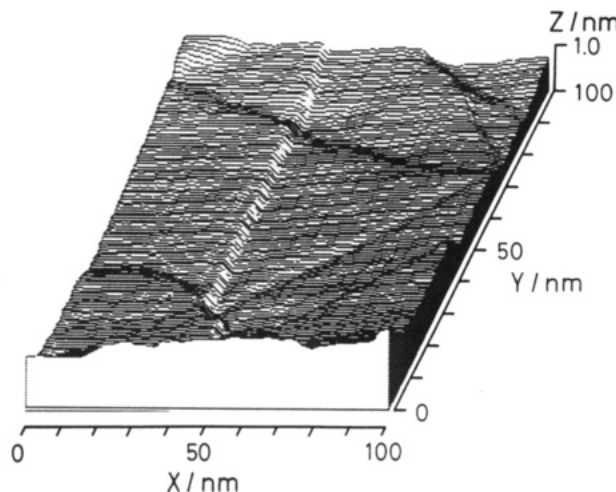


Figure 2. STM image of a Pt(111) surface in 0.05 M H_2SO_4 . Reprinted with permission from ref 19. Copyright 1990 American Institute of Physics.

passes between the substrate and the counter electrodes. For *in-situ* STM, the electrode potential of the tip is maintained within certain regions to minimize faradaic processes at the tip/solution interface. The tip can be continuously scanned over the substrate surface, even when electrochemical reactions take place at the working electrode, although a screening effect of the tip for the diffusion of reactants in solutions must be considered. Several examples of *in-situ* STM studies of electrode/electrolyte interfaces follow.

Well-Defined Metal Surfaces. A large number of electrochemical investigations of structure-sensitive redox reactions have been performed on various electrodes using single crystals with well-defined surfaces.¹⁷ Several experiments have been performed on single-crystal electrodes to establish *in-situ* STM as an electrochemical tool having atomic resolution. The first use of *in-situ* STM was in the study of the surface of HOPG.¹² Single atomic steps on Au(111) could also be seen in an electrolyte solution.¹⁸ Similar atomically resolved images have been achieved on other metals, such as Pt, Rh, Pd, and Ag.

Figure 2 shows a typical STM image of a $1000 \times 1000 \text{ \AA}$ area of Pt(111) in an aqueous sulfuric acid solution.¹⁹ The heights of the steps are in accordance with monatomic step heights of ca. 2.4 \AA , and the orientations of the steps differ by 60° as expected for a surface with the threefold symmetry of the (111) surface. The atomically flat (111) terraces usually extend over a few hundred angstroms, demonstrating that the surface examined has a long-range order with a low density of defects. Atomically flat and clean surfaces must be prepared to obtain atomic information about the surface structure with STM. Such surfaces can be obtained from polished single crystals, by the "flame-annealing quench technique",²⁰ and by vacuum evaporation on suitable substrates.

Structural Change. Reconstruction of surfaces to minimize the surface free energy is a well-known occurrence in UHV studies. The reconstruction of Au electrodes in aqueous solutions using UHV electrochemical systems has long been discussed. Very recently, however, evidence for the surface reconstruction has been revealed by *in-situ* STM studies. For example, the Au(110) (1×1) structure is transformed to (1×2) and (1×3) structures in the double-layer region by lowering the electrode potential to -0.3 V vs SCE in a HClO_4 solution as shown in Figure 3.^{21,22} It is important to compare structures of reconstructed surfaces in UHV and those in solution to understand better the role of electronic structure of the electrode surface in solution.

The structural changes of surfaces during oxidation-reduction cycles can also be studied by *in-situ* STM. Island formation has been observed on an atomically flat Pt(111) surface after applying

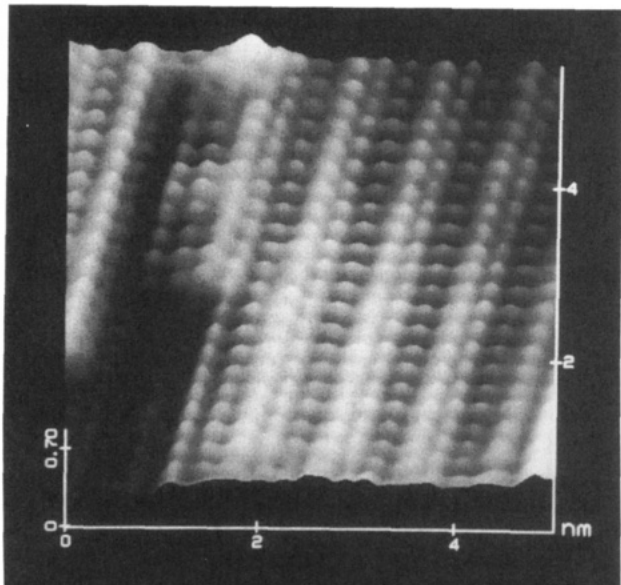


Figure 3. STM image of a reconstructed Au(110) surface having (1×2) symmetry in 0.1 M HClO_4 .²¹

potential cycles.¹⁹ Simultaneous formation of islands and pits of monoatomic height has been found on Au(100) after a potential cycle.²³ Roughening, annealing, and dissolution have been reported to accompany the oxidation-reduction of the Au(111) surface,²⁴ indicating that the surface diffusion of Au was 2–3 orders of magnitude faster in solutions containing chloride ions. Similarly, STM can be used to follow changes in the surface of HOPG during oxidation.²⁵ Structural changes, such as those described above, can be very important factors in the understanding and control of electrochemical dissolution and deposition processes at various metals, alloys, and other electrodes.

Underpotential Deposition. The electrochemical deposition of metal adlayers on a foreign metal substrate is one of the most structure-sensitive reactions that occur at the electrode/electrolyte interfaces.²⁶ There are many systems where the first monolayer is deposited at potentials more positive than the reversible (Nernst) potential of the respective bulk phase; this is called underpotential deposition (UPD). The UPD of metals, as well as the adsorption of hydrogen, has been investigated extensively on single-crystal electrodes of different orientation. UPD processes are indeed important in revealing the role of surface structure on the electrochemical reaction.

STM images of individual copper adatoms have recently been resolved,^{27–29} demonstrating that the structure for the first UPD layer of Cu on Au(111) in an aqueous sulfuric acid solution is $(\sqrt{3} \times \sqrt{3})R30^\circ$. A (5×5) structure was also observed in the same solution in the presence of chloride,²⁷ suggesting that the coadsorption of anions is an important factor in determining the structure of UPD adlayers. *In-situ* AFM has also been employed to study, with atomic resolution, the UPD of Cu,^{30,31} Bi,³² and Hg³³ on Au(111).

Figure 4 shows a cyclic voltammogram for the UPD of Cu on Au(111). Two different waves for the UPD of Cu can be seen in the potential region between 0.35 and 0 V vs SCE before the start of bulk deposition. The image acquired at 0.4 V vs SCE, where no Cu UPD has taken place, indicates that the Au(111) surface has a (1×1) structure under these conditions. After achieving atomic resolution of the substrate surface at 0.4 V, the electrode potential was scanned cathodically and was held at 0.2 V, between the two UPD peaks. A very clear STM image with corrugation heights of 0.5–0.7 Å was observed as shown in Figure 5. The distance between nearest neighbor Cu atoms is about 4.8 Å. The atomic rows of Cu are at an angle of 30° relative to the

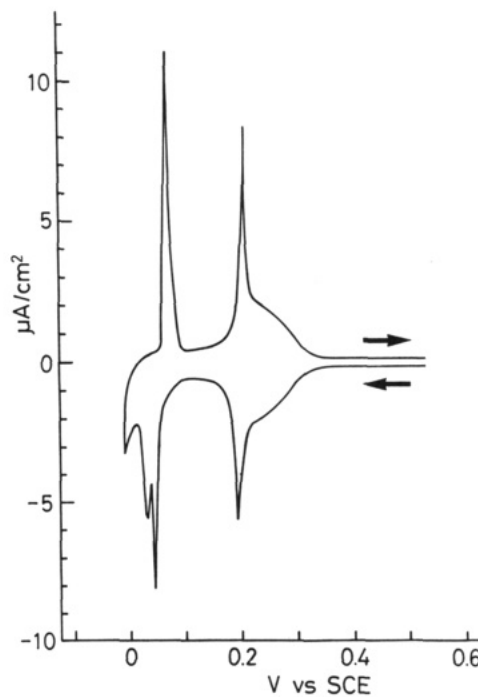


Figure 4. Cyclic voltammogram for UPD of Cu on a Au(111) electrode in 0.05 M H_2SO_4 + 1 mM CuSO_4 solution.²⁹

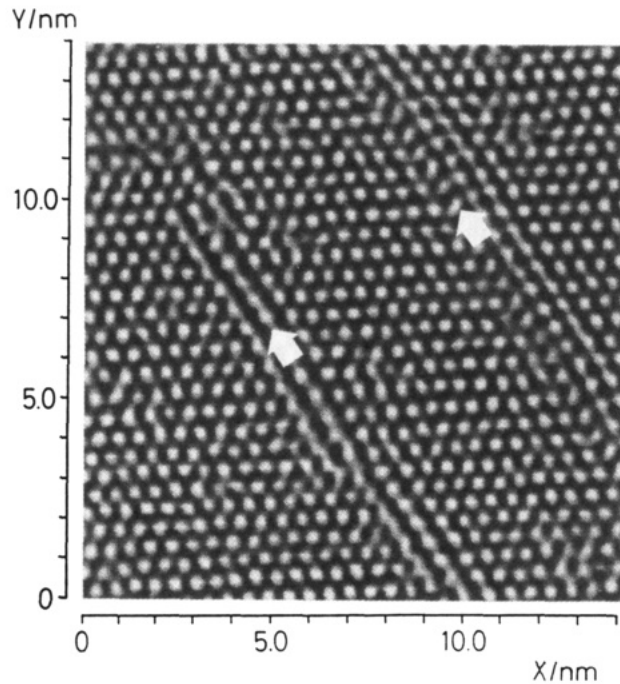


Figure 5. STM image of the first Cu adlayer. Arrows indicate phase boundaries.²⁹

underlying Au lattice. These observations show that the structure of the first Cu adlayer is $(\sqrt{3} \times \sqrt{3})R30^\circ$. However, interesting phase boundaries are often observed in images acquired on larger scan areas, as shown in Figure 5.²⁹ Two $(\sqrt{3} \times \sqrt{3})R30^\circ$ domains are simply shifted by a half position, suggesting that the adsorption of Cu occurs almost equally on two nonequivalent threefold hollow sites on Au(111).

The same $(\sqrt{3} \times \sqrt{3})R30^\circ$ structure has been found for the first layers of the UPD of Cu on Pt(111)³⁴ and of Ag on Au(111)³⁵ in aqueous sulfuric acid solution. The appearance of the widely spaced $(\sqrt{3} \times \sqrt{3})R30^\circ$ structure is probably due to the presence of anions, such as SO_4^{2-} and HSO_4^- , on the surface. The role of the coadsorbed anions is important to the understanding of the UPD processes.³¹

Molecular Adsorbates. The structural determination of chemisorbed atoms and molecules on metal electrodes is another important application. STM studies have been carried out for iodine and bromine adsorbed on Pt(111)³⁶ and Au(111),^{37,38} respectively. Sulfide adsorption also yields ordered ($\sqrt{3} \times \sqrt{3}$)-R30° layers.³⁹ *In-situ* IR spectroscopy has been successfully combined with STM to characterize the CO adlayers on Rh-(111) and Pt(100) electrodes in aqueous solutions.^{40,41} Substrate-induced ordering of monolayers of $[(\text{Ru}(\text{bpy})_2(\text{bpy}-\text{CH}_2)_x-\text{bpy})]^{2+}$ on reconstructed Au(III) surfaces in dimethylformamide solutions has been studied by STM.⁴² STM studies may also be important in characterizing organized monolayers on electrode surfaces, such as those employed in dynamic studies described below.⁴³⁻⁴⁵ The above results have accelerated further investigations to resolve chemisorbed molecular species on electrodes in electrolyte solutions, which complement the extensive studies of electrodes using the UHV electrochemical system.⁴⁶

Semiconductor Electrodes. Surface topographic images of semiconductors such as *n*-TiO₂, *n*-ZnO, GaAs, Ge, and Si have been acquired in aqueous solutions usually without atomic resolution mainly because of the difficulty in the preparation of a well-defined semiconductor surface. However, there are numerous examples of atomic-resolution STM in studies of semiconductors in UHV.⁴⁷ STM has recently been used to image, in aqueous HF solutions, Si(111) terminated with monohydride (Si(111):H-1×1) prepared by chemical and electrochemical wet etching.^{48,49} Wet etching of semiconductors, particularly of Si, is important in LSI technology, and detailed STM studies of chemical processes that occur during etching should be important in the future.

In-situ STM can also be applied to the determination of band structures at semiconductor/liquid interfaces. Electron tunneling between the conduction or valence bands in the semiconductor and levels in the tip depends upon the potential difference between the semiconductor and the tip. Measurements of tunneling current as a function of bias, as well as tunneling spectroscopic investigations of work function and differential conductivity (dI/dV) of semiconductor interfaces, will be useful in mapping the energy levels of bands and surface states.⁵⁰⁻⁵²

(b) *Ultramicroelectrodes and Scanning Electrochemical Microscopy.* An ultramicroelectrode (UME) is an electrode whose smallest dimension is in the micrometer (μm) range. Indeed, disk-shaped electrodes with 1- μm diameters are now routine, and several reports have described much smaller electrodes with dimensions of the order of nanometers. Electrode shapes comprise disks, rings, bands, and interdigitated arrays. Such electrodes can be applied to electrochemical studies of the same type as those carried out at much larger electrodes at the same current densities. However, several advantages arise from the use of very small electrodes: (i) The absolute currents with these electrodes are very small, usually in the pA-nA range. Thus, even with highly resistive solvents, the uncompensated resistive drop (iR_u) that perturbs accurate potential measurements is small. This allows a whole range of new media, such as nonpolar solvents and supercritical fluids, to be investigated by electrochemical methods. For example, the recent work on the electrochemistry of the fullerenes in solvents such as benzene employed ultramicroelectrodes.⁵³ Similarly, ultramicroelectrodes are needed in studies of electrolytes like supercritical water⁵⁴ and high-resistance solid electrolytes. (ii) The very small size of such electrodes allows them to be employed as high-resolution probes, for example, in the scanning electrochemical microscope (SECM) discussed below or as sensors in biological systems (single cells, synapses). (iii) Arrays of UMEs are convenient as analytical sensors and as substrates for the construction and characterization of devices based on modified electrode surfaces. Moreover, UMEs have two characteristics which make them particularly useful in dynamic studies, as described in section III.B.1: (iv) The rate of

mass transfer by diffusion to such an electrode is very high. For example, the mass-transfer coefficient for a UME is of the order of D/r (where D is the diffusion coefficient and r the electrode radius), so the mass transfer to a $r = 1 \mu\text{m}$ electrode (ca. 0.5 cm/s) is faster than the convective transport to a rotating disk at a rotation rate of 10⁴ rev/min. This high mass transfer makes possible measurements of very large rate constants, e.g., those for heterogeneous electron transfer at the electrode/electrolyte interface under steady-state conditions. (v) UMEs are characterized by very small double-layer (dl) capacitances (C_d) of the interface and, hence, small time constants ($R_u C_d$) for dl charging. This allows measurements in a very short time regime (as discussed in section III.B.1), e.g., by rapid cyclic voltammetry, and makes possible transient studies of rapid heterogeneous and homogeneous reactions. The background, methodology, and applications of UMEs have been reviewed.^{55,56}

Ultramicroelectrodes will continue to be useful in characterizing the electrode/electrolyte interface and in studies of electrochemical systems. Projected applications include (i) studies of electrodes with sizes approximating molecular dimensions.⁵⁷ Such electrodes could show quantum and unusual mass-transfer effects. They may also be useful in the observations of stochastic events. (ii) Small interdigitated arrays (IDA) and related structures can be employed in the fabrication of electrochemically based "molecular" electronic devices and sensors. (iii) Studies of the electrode/electrolyte interface with novel electrolyte media—solids, supercritical fluids, nonpolar solvents, perhaps even gases—are important, as are (iv) studies of single molecular events at electrode surfaces (e.g., nucleation, pore formation, adsorption, deposition). (v) The development of ultramicroelectrodes with well-defined single crystal surfaces would be desirable.

Scanning Electrochemical Microscopy. The scanning electrochemical microscope (SECM) uses STM technology to position and move an ultramicroelectrode probe (tip) near a substrate surface. In SECM, the faradaic current produced by a redox reaction at the tip is perturbed by the presence of a substrate, which can be either an electronic conductor or insulator, and this perturbation can be employed to obtain topographic images and information about reactions at the substrate surface or within the solution in the gap between tip and substrate. The resolution obtained with the SECM depends upon the dimensions of the ultramicroelectrode tip employed. Currently, the best resolution reported is in the range of 50 nm. Several reviews discuss the principles, apparatus, and applications of SECM.^{58,59}

Some particular applications of the SECM in characterizing the electrode surface include the following: (i) The SECM can image arrays or composites consisting of both conductive and insulating regions and can indicate the conductive nature of regions. As opposed to imaging by optical microscopy, portions of the conductive surface just below the insulating surface are not imaged. (ii) The SECM can also be employed to distinguish regions of different reactivity ("reaction rate imaging") on an electrode surface. (iii) Films on electrode surfaces can be probed with nanometer resolution by measuring the tip current as the tip passes through the film.⁶⁰ (iv) Adsorption equilibria and kinetics on electrode (and insulator) surfaces can be studied. (v) Rapid reactions that take place in the solution immediately above the electrode surface in the microscopic cell defined by the tip area and the tip-substrate gap can be studied. (vi) High-resolution fabrication by deposition, etching, and electrosynthesis has been demonstrated with the SECM. (vii) The structure of porous synthetic⁶¹ and biological⁶² membranes (e.g., human skin) can be imaged by measuring the rate at which redox species emerge from individual pores.

A number of additional applications of the SECM can be envisioned. (i) New probes, such as specific ion and enzyme electrodes, can be used as tips. These would allow identification of species, e.g., protons and peroxide, produced at the electrode

surface. (ii) The semiconductor/electrolyte interface can be used in a photoelectrochemical mode to generate species by light pulses. The time-of-flight of such species to the tip and the measured tip response can be employed to determine diffusion coefficients and reaction rate constants. (iii) The tip can be used to penetrate bilayers, membranes, and polymer films on electrode surfaces and to measure their thickness and the electrochemistry of species within the layers. (iv) High-resolution fabrication on electrode surfaces may be possible via modification of self-assembled monolayers and Langmuir-Blodgett (LB) films.

(c) *X-ray Methods*. Because of their penetrative power through condensed phases and their short wavelengths, X-rays are well studied for *in-situ* studies of buried interfaces. The relatively weak interaction of X-rays with matter, however, means that powerful X-ray synchrotron sources are required for many of these studies. Synchrotron sources offer a broad spectral range of polarized, highly collimated X-rays with intensities that are 10^3 - 10^6 higher than those of a conventional X-ray tube. Third-generation synchrotron sources, such as the advanced photon source, are being built, and their projected 10^4 increase in brightness will allow for fundamentally different experiments to be performed including the study of dynamic processes. There are a number of X-ray-based techniques that can be employed in the *in-situ* study of electrochemical interfaces.^{63,64} These include surface extended X-ray absorption fine structure (SEXAFS), X-ray standing waves (XSW), surface diffraction, and reflectivity measurements.

SEXAFS. EXAFS (extended X-ray absorption fine structure) refers to the modulations in the X-ray absorption coefficient beyond an absorption edge and involves the measurement of the absorption coefficient (or any parameter that can be related to it) as a function of photon energy.⁶⁵⁻⁶⁷ These modulations arise as a result of the interference between the outgoing wave (due to the photoionization of a core-level electron upon absorption of an X-ray photon) and a backscattered wave due to the presence of near neighbors (typically $\leq 5 \text{ \AA}$; EXAFS is only sensitive to short-range order). The modulations present at energies from about 40 to 1000 eV beyond the edge are termed EXAFS. To a good approximation, the frequency of the EXAFS oscillations depends on the distance between the absorbing atom and its near neighbors, whereas the amplitude of the oscillations depends on the numbers and type of neighbors, as well as their distance from the absorbing atom. From an analysis of the EXAFS data, one can obtain information on near-neighbor distances ($\pm 0.02 \text{ \AA}$), numbers ($\pm 15\%$), and types. Further advantages of EXAFS are the following: (i) it can be applied to all forms of matter; (ii) for solid samples, single crystals are not required (EXAFS yields short-range-order information); and (iii) by choosing the X-ray energy, one can focus on the environment around a particular element. Furthermore, the energy of the absorption edge can indicate the effective oxidation state of the absorbing atom. Although more difficult to interpret, because of multiple scattering effects, the near-edge region of the spectrum is very rich in structural information.

EXAFS and SEXAFS have been employed in the study of electrochemical interfaces with emphasis on underpotential deposition (UPD), metal oxides, corrosion, and others.⁶⁸⁻⁷³ Especially notable findings in the study of UPD systems have been the elucidation of well-defined structures of the metal adlayers and their coverage dependence. Particularly surprising has been the observation of strong scattering by adsorbed solvent and supporting electrolyte, suggesting a very strong interaction of these interfacial species with the metal *adlayer*. The use of well-defined bulk single-crystal electrodes and improved cell designs has further enhanced the applicability of this technique.

In terms of future developments, the use of dispersive methods appears most exciting.⁷⁴ In conventional experiments, EXAFS spectra are measured by scanning a monochromator so that the

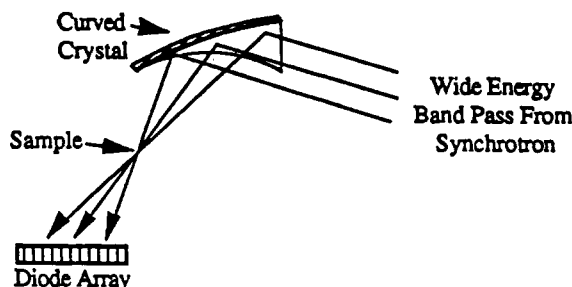


Figure 6. Depiction of an energy dispersive arrangement for X-ray absorption spectroscopy.

absorption coefficient is measured at a single energy at a time, with the acquisition of a single spectrum taking about 30 min. An alternative is to employ a dispersive approach where a beam with a broad energy distribution (500–1000 eV) is brought to a tight focus (about $50 \mu\text{m}$) on a sample by the use of a curved crystal (Figure 6). Beyond the sample, the X-ray beam fans out according to energy. If a photodiode array is placed at an appropriate distance, all of the energy components of the beam can be measured at the same time. In this approach, there is a gain of 2–3 orders of magnitude in terms of data collection rate. Such an approach allows time-dependent measurements to be carried out. Millisecond time resolution has been demonstrated, and this value could be decreased by a few orders of magnitude with the new synchrotron light sources, thus providing time resolution that is appropriate to a number of dynamic processes. Especially relevant applications of this technique would include dynamic studies of polymer films on electrodes. Achieving monolayer sensitivity is rendered difficult in this approach, since the attenuation of the beam would be very low. However, monolayer surface sensitivity could, in principle, be achieved by carrying out REFLEXAFS⁷⁵-type measurements where the relevant information is contained within the reflected beam.

X-ray Diffraction. X-ray diffraction (XRD) is the most powerful method to study the structure of crystalline materials; its application to electrochemical interfaces has provided detailed information on the atomic structure both of the electrode surface and that of adsorbed layers.⁷⁶⁻⁸⁶ A special case of X-ray diffraction has been termed surface X-ray diffraction (SXRD) or grazing incidence X-ray scattering (GIXS). In this technique, the X-ray beam is incident on the surface at an angle just above the angle of total external reflection (typical angles of incidence are 0.2–0.5°). The diffracted beam is measured at an angle 2θ from the specularly reflected beam. In this geometry, the scattering vector is predominantly in the plane of the surface and hence is most sensitive to in-plane structure. Two examples will be presented, the observation of potential-induced reconstruction of Au(111) and the determination of the structure of an underpotentially deposited monolayer, to illustrate the power of this technique.

Au(111) reconstructs in vacuum, and from anomalies in measurements of capacitance a similar reconstruction, reversibly induced by the application of potential, has been proposed.⁸⁷ This has recently been observed using SXRD. Figure 7 shows the observed scattering intensity from a Au(111) surface in 0.01 M NaCl versus the scattering vector scanning through the (0,1) reflection along the (1,1) direction at several applied potentials. At 0.10 V, only scattering from the unreconstructed Au surface is observed. At more negative potentials, the intensity of the scattering from the reconstruction ($q = 0.038$) is clearly seen to grow. From this⁸⁶ and other in-plane scattering data, the reconstruction can be unambiguously shown to be the same (p×23) reconstruction observed in vacuum (although the long-range herringbone pattern does not form).

The structures of several underpotentially deposited monolayers have been determined. An illustrative example is the monolayer of Bi which forms on Ag(111).⁷⁶ Diffraction peaks from the

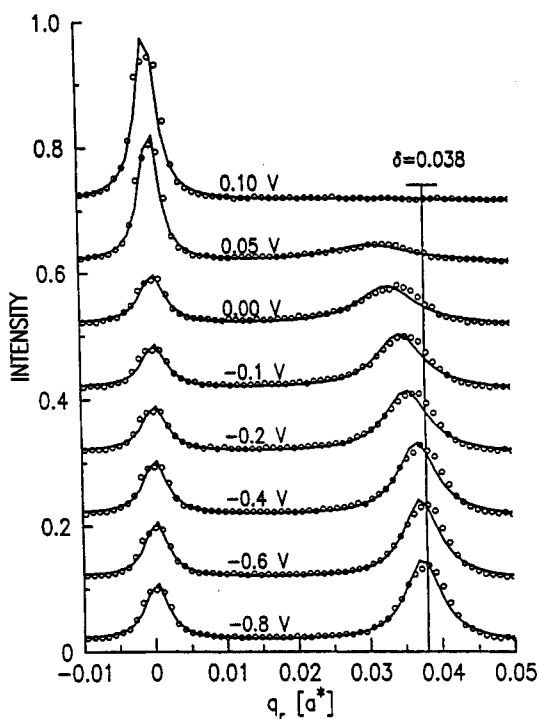


Figure 7. Representative X-ray scattering profiles along the q_r axis at $L = 0.2$ in 0.01 M NaCl solution at a series of potentials chosen from scans between 0.1 and -0.8 V in steps of -0.05 V. The solid lines are fits to a Lorentzian line shape.⁸⁶

monolayer are shown in Figure 8 and the corresponding structure in Figure 9A. This structure is somewhat unique in that it is incommensurate along the Ag[01 $\bar{1}$] direction but commensurate along the Ag[211] axis. A manifestation of this is seen in the two-dimensional (2D) isothermal compressibility of the Bi layer as shown in Figure 9B. Along the Ag[01 $\bar{1}$] axis, the Bi monolayer is seen to compress as the potential is made more negative. This same phenomenon is observed for all of the incommensurate monolayers that have been studied to date and is a result of the thermodynamic driving force to pack more Bi atoms on the surface. These data have provided the only measurements of the 2D compressibility of metals. Although the Bi compresses along the Ag[01 $\bar{1}$] axis, the distance between Bi atoms along the Ag[211] axis does not change with potential, because the Bi atoms maintain their registry with the Ag substrate along this axis. The fact that the first monolayer electrochemically deposited is often very compressed relative to the bulk explains why electrochemical heteroepitaxy is rarely observed.⁷⁸

While the above discussion has focused on obtaining information about lattice spacings in the plane of the surface, one can also probe the electron density normal to the surface. The technique to accomplish this is based on measuring changes in the intensities of crystal truncation rods (CTR).⁸⁸ Although the details are beyond the scope of this brief review, it is the abrupt termination of a crystal which results in streaks of intensity that connect Bragg points along directions normal to the surface. By carefully measuring the profiles of these streaks of intensity, one can determine the roughness of the surface and the details of the registry of an overlayer. Indeed, using this technique, one can observe the slight expansion in the lattice spacing (normal to the surface) of the top layer of atoms.

While the examples above all refer to measurements of static structure, dynamic processes may be probed as well. To date, only relatively slow surface processes, such as the kinetics of the reconstruction of the Au(111) surface, have been followed.⁸⁶ The elucidation of dynamic properties and the structure of water and ions in the double layer are problems which can now be approached, with new synchrotron sources, such as the advanced photon source.

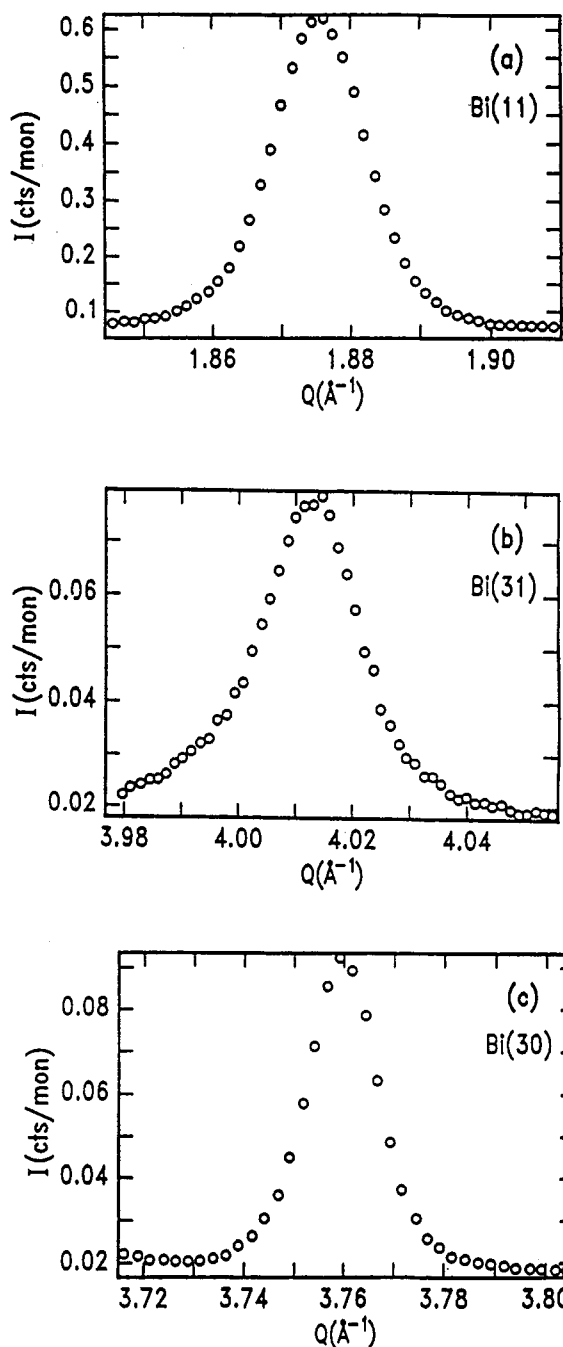


Figure 8. *In-situ* X-ray diffraction scans from a Bi monolayer on Ag(111). The ordinate is the number of counts received by the detector normalized by the monitor counts. (a) Bi(11) peak, (b) Bi(31) peak, (c) Bi(30) peak. From ref 76.

Reflectivity Measurements. The measurement of X-ray reflectivity of an interface can provide the electron density profile in a direction normal to the interface. Thus, it is very sensitive to roughness as well as to variations produced by phenomena such as surface reconstructions. For small angles of incidence, variations in the reflectivity can be represented as a perturbation from that predicted by the Fresnel law of optics for a perfect abrupt interface.

In the Born approximation limit, the ratio of the measured reflectivity $R(\Theta)$ to the Fresnel reflectivity $R_F(\Theta)$ yields the average electron density gradient along the surface normal and is given by

$$\frac{R(\Theta)}{R_F(\Theta)} = \left| \frac{1}{\langle \rho_e \rangle} \int_{-\infty}^{\infty} \left\langle \frac{\partial \rho_e}{\partial z} \right\rangle e^{iQ_z z} dz \right|^2 \quad (1)$$

X-ray reflectivity measurements have been used in the study of

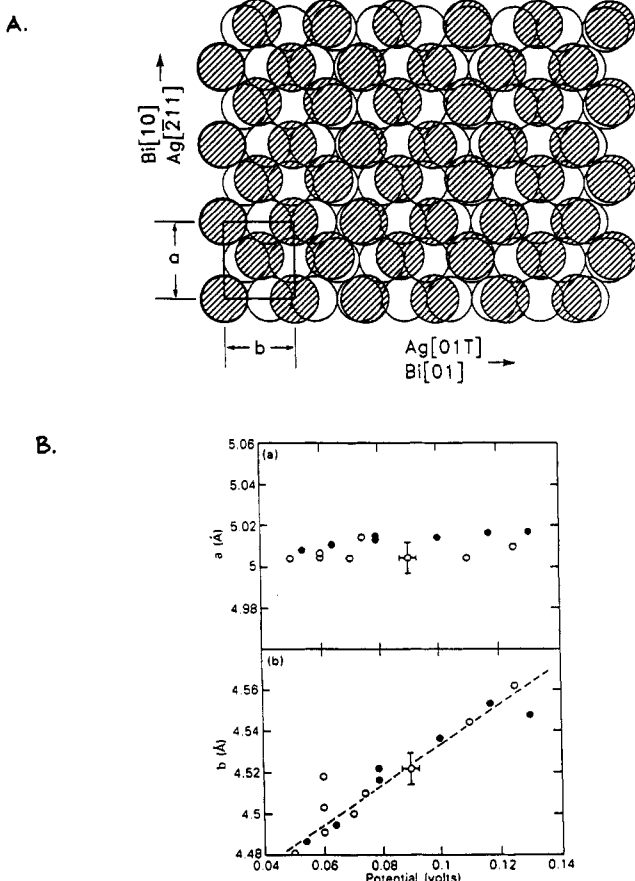


Figure 9. (A) *In-situ* structure of Bi/Ag(111). The open circles represent the surface atoms of the Ag substrate (with hexagonal symmetry), and the shaded circles represent the Bi adatoms. The relative sizes correspond to the near-neighbor spacing of bulk Ag (2.89 Å) and bulk Bi (3.07 Å). The Bi monolayer is commensurate in the *a* direction (*a* = 5.005 Å = $\sqrt{3}$ times Ag nearest-neighbor distance) but is incommensurate in the *b* direction (*b* = 4.48–4.56 Å). (B) Dependence of the Bi monolayer lattice constants on the applied potential (*V*). The filled and open circles are for chloride-free and chloride-containing electrolytes, respectively. (a) The lattice constant *a*. The average value is *a* = 5.007 ± 0.002 Å, demonstrating that the Bi monolayer is uniaxially commensurate with the Ag surface. (b) The lattice constant *b*. The line is a linear least-squares fit to the data and has a slope $db/dV = 0.95 \pm 0.05$ Å/V.⁷⁶ From ref 76.

surface reconstructions on single-crystal electrode surfaces as well as in the study of oxides.

X-ray Standing Waves. The X-ray standing wave (XSW) technique represents an extremely sensitive tool for determining the position and coherence of adsorbates as well as the distribution of interfacial species.⁸⁹ This technique is based on the X-ray standing wave fields that arise as a result of the interference between coherently related incident and reflected waves, either by total external reflection or Bragg diffraction (Figure 10). The period of the standing wave is given by

$$D = \lambda/2 \sin \Theta \quad (2)$$

where 2Θ is the relative angle between the waves. If the angle of incidence is increased, the value of $2 \sin \Theta$ increases and thus the period of the standing wave decreases. In addition, the standing wave can be moved with respect to position by changing the relative phase between the incident and reflected waves. Thus, the standing wave can be made to sample an adsorbate or overlayer at varying positions above the substrate interface. By judicious choice of experimental parameters, one can vary the characteristic length scale of the technique to be from a few to hundreds of Å, and this covers the range of distances of relevance to electrochemical interfaces.

XSW studies of electrochemical interfaces include the underpotential deposition of metal monolayers such as Tl on Cu^{90,91}

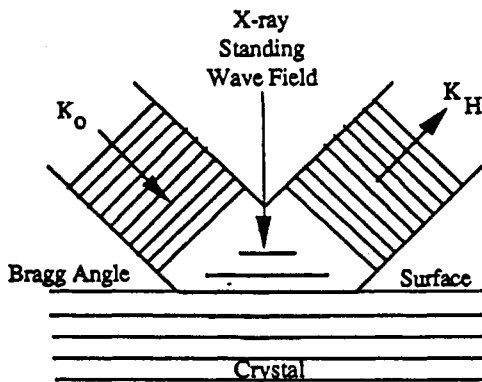


Figure 10. Depiction of the formation of an X-ray standing wave field as a result of the interface between incident and reflected plane waves.

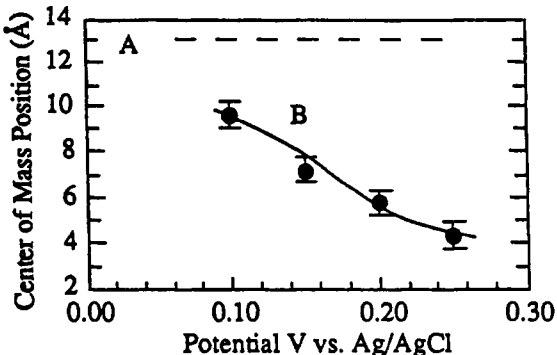


Figure 11. Comparison of data (points) for the electrodeposition of copper on an iodine-treated platinum surface with the predictions from models based on (A) statistical occupancy of surface sites and (B) progressive occupancy of surface sites beginning with the deepest.

and Cu on Pt.⁹² In addition, studies of potential-dependent structural and distributional changes, such as iodine on platinum, have been carried out.⁹³ For example, the mechanism of the underpotential deposition of copper on an iodine-treated platinum surface from a Pt/C layered synthetic microstructure (LSM) has been studied.⁹⁴ XSW measurements under total external reflection and Bragg diffraction conditions as a function of surface coverage of copper, as well as potential-dependent changes in the position of the center of mass of the copper layer, could be determined. One can envision two limiting cases in terms of the mechanism of deposition. If open surface sites were occupied in a random mode, one would expect a homogeneous copper distribution whose center of mass was always at the same *z* position, namely, the center of the Gaussian representing the surface site's concentration profile (i.e., the position with the largest density of open sites). The second model is one in which open surface sites are occupied sequentially with the deepest ones first. In this case, the center of mass position would vary with the copper surface coverage. Both of these models are plotted, along with the experimental data, in Figure 11 as a function of potential. Clearly, the observed results are in excellent agreement with the model that involves sequential filling (Figure 11, curve B) of available surface sites. This implies that the more favorable surface sites for deposition are the ones closest to the platinum bulk lattice, either because the substrate-deposit interactions are maximized at these sites or because the interaction with the electric fields present at the interface is greatest at these locations. This type of study illustrates the power of the XSW technique for the *in-situ* study of electrochemical interfaces. Perhaps the greatest advantage of XSW measurements is that they can provide information on the distribution, with angstrom resolution, of species close to but not in contact with a surface. The main drawbacks of XSW experiments are that they are experimentally demanding and that they require nearly perfect crystals. However, the use of a back-reflection geometry allows for the use of high-

quality (though not perfect) single crystals. In addition, the technology for the preparation of LSM has developed to a level where a single crystalline layer can be deposited. These advances may open up this technique to more general use.

(d) *Nonlinear Optical Methods*. The most extensively investigated of the nonlinear optical techniques at electrode surfaces is second harmonic generation (SHG),⁹⁵⁻⁹⁸ where the electrode surface is irradiated with a pulsed laser and light at twice the frequency of the fundamental frequency of the laser is collected near the reflected angle. The attractiveness of this technique is that it is inherently surface selective (as are all second-order nonlinear processes), because the process which leads to frequency doubling is forbidden in the bulk of centrosymmetric crystals but is allowed at the surface where this inversion symmetry is broken. The second harmonic response from the metal electrode is large compared to that from any overlayer, so this technique is primarily sensitive to the properties of the crystal surface. The intensity of the frequency-doubled light depends on the surface nonlinear susceptibility, which is sensitive to the charge on the surface, the presence of adsorbates, and surface morphology. One of the most exciting developments in this area has been the observation of an anisotropy in the nonlinear response of single-crystal metal electrodes with the rotation of the crystal about its surface normal. This surprising result opens the way for using SHG to probe the geometric structure of the electrode as well as the registry of deposited overlayers, as this is observed to affect the rotational anisotropy.⁹⁹ More recently, this anisotropy has also been shown to be markedly affected, when the fundamental or doubled frequency is near a transition between states or bands of the electrode surface¹⁰⁰ (resonant SHG), as shown in Figure 12. This promises to be a fruitful technique for providing information on the electronic structure of the electrode.

More fundamental work directed at understanding the SHG response is required before this technique will be used as a routine method for determining the structure of electrodes, adsorbed layers, or electronic properties. Developing this understanding will be the key challenge in this area over the next several years. Two other nonlinear optical techniques, while far less developed, also show considerable promise: sum frequency generation (SFG) and hyper Raman spectroscopy (HR). Both of these techniques probe vibrational transitions at surfaces. Hyper Raman is similar to SHG except that instead of measuring the intensity of light produced at twice the frequency of the incident light, $2\omega_i$, one measures the intensity produced at $2\omega_i - \omega_v$, where ω_v corresponds to the frequency of a vibrational transition at the surface. The hyper Raman effect is approximately 5 orders of magnitude weaker than normal Raman. In SFG, an infrared wave ω_{IR} is mixed with visible light ω_i at the surface to produce visible light at $\omega_i + \omega_{IR}$. The frequency of the infrared laser is scanned, and when the infrared wave is in resonance with a vibrational transition the intensity of the mixed wave is increased. Since the mixing only occurs at the surface, this technique is less sensitive to absorption in the bulk than infrared reflection spectroscopy.

2. *UHV (ex-situ) Electrochemical Techniques*. The application of UHV techniques requires that the characterization be performed outside the electrochemical cell. The possibility of structural and compositional changes upon removal (emersion) of the electrode from solution limits the scope of the UHV-EC approach.¹ Its enormous advantage is that, once the sample is in vacuum, any number of analytical techniques can be used to study the surface. Several hundred papers have appeared over the past two decades that describe electrochemical phenomena examined by UHV-based methods at polycrystalline electrodes; studies of single-crystal electrodes are more recent. The number of researchers presently involved in UHV-EC studies of the electrode/electrolyte interface has increased over the past few years. The interfacial structures derived from UHV-EC work

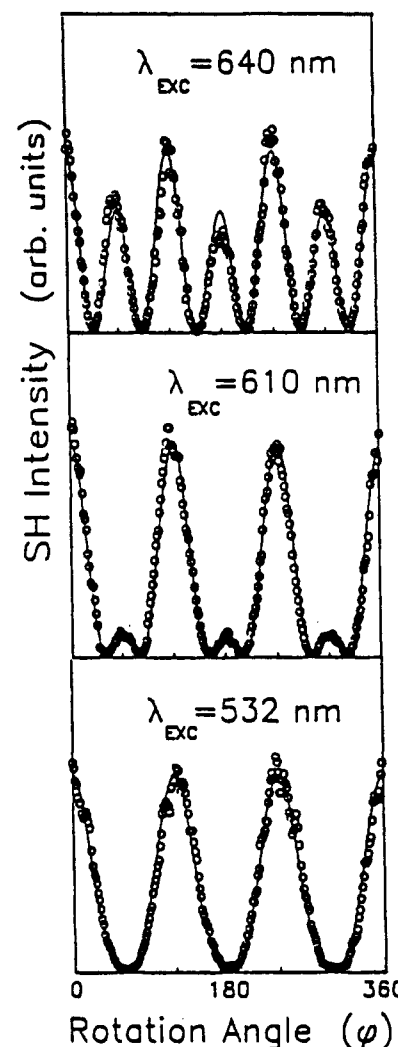


Figure 12. The *p*-polarized SHG as a function of azimuthal rotational angle for Ag(111) in 0.1 M NaClO₄ under *p*-polarized excitation at the indicated wavelengths. From ref 100.

have provided much of the impetus in the development of the *in-situ* methods described above.

Vacuum-based techniques that have been employed for the characterization of electrode surfaces include the following:^{1,101-104} low-energy electron diffraction (LEED) and reflection high-energy electron diffraction (RHEED) for surface crystallography, Auger electron spectroscopy (AES) and X-ray photoelectron spectroscopy (XPS) for surface composition and chemical bonding information, high-resolution electron energy loss spectroscopy (HREELS) for surface vibrational spectroscopy, work function-change measurements for interfacial electronic properties, and thermal desorption mass spectrometry (TDMS) for adsorption energetics. Other methods that do not require high vacuum, such as IRAS and SHG, have also been used to examine the electrode surface emersed into UHV.

Several significant advances have been achieved over the past few years that further reinforce the usefulness of the UHV-EC approach. Foremost among these are (i) the attainment of ultraclean conditions in the transfer of the electrode between the UHV and EC chambers, (ii) a better understanding of the emersion process, and (iii) the verification of UHV-EC-derived structures by *in-situ* methods. A related development concerns the "synthesis" of the electrochemical double layer in UHV by sequential cryogenic adsorption of its solvent-electrolyte-adsorbate constituents.^{105,106}

UHV-EC investigations with monocrystalline electrode surfaces can be broadly classified into three groups. The first emphasizes

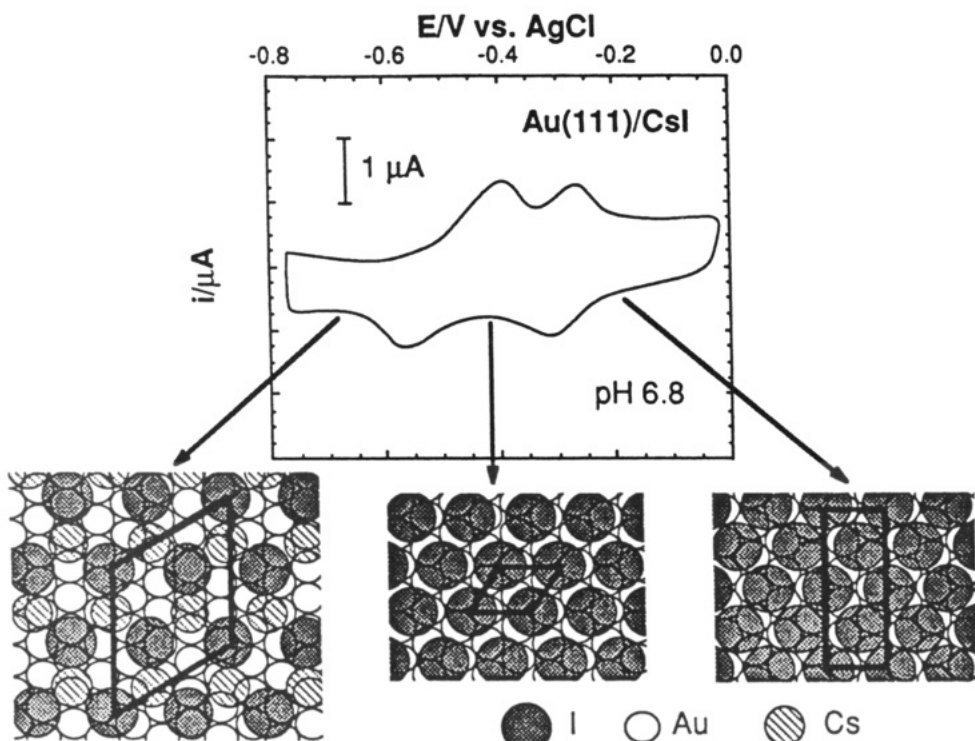


Figure 13. Cyclic voltammogram and interfacial adlayer structures: Au(111) in dilute CsI at pH 6.8. The structures were derived from LEED and AES data. From ref 112.

the structure and constitution of the double layer. The second centers on electrodeposition reactions, including hydrogen and oxygen adsorption. The third deals with the structure and reactivity of chemisorbed molecules.

Electrical Double Layer. Two general strategies have been adopted. One, strictly a model approach, involves the layer-by-layer synthesis of the double layer by cryogenic adsorption;^{105,106} the “control” of electrode potential is based upon coadsorption of species such as H₂ or K. The other approach is based upon direct characterization of the electrolyte layer immediately after emersion. In the ideal emersion process, the electrode contains an interfacial layer identical in composition and structure to that of the electrode when it was in solution. The optimum conditions for such emersion have been mapped out.^{107–109} The existence of an emersed double layer has been established. The stability, structure, and composition of emersed layers obtained under various conditions have been documented. UHV-EC studies of specifically adsorbed anions have been carried out at Pt(111), Pt(100), stepped Pt(s)[6(111)×(111)], Cu(111), Ag(111), Au(111), and Pd(111) electrodes. The anions studied include monatomic species such as Cl⁻, Br⁻, and I⁻ and polyatomic species such as SH⁻, CN⁻, SCN⁻, and SO₄²⁻.¹

Underpotential Electrodeposition. UHV-EC studies of UPD can be categorized according to whether the experiments were used to correlate the substrate structure with the UPD voltammograms or to determine the resultant interfacial properties of the adatom-modified substrate. Investigations devoted to structure–voltammetry relationships help establish reference states; those focused on postdeposition analysis yield important information concerning the electrocatalytic selectivity of mixed-metal interfaces.

The first applications of combined LEED, AES, and EC involved the correlation of the surface crystallographic orientation with the underpotential hydrogen deposition at Pt electrodes. By current standards, those initial studies are not definitive because of the lack of a rigorous control of substrate structure and the use of multiple surface oxidation–reduction cycles to generate a clean, *but structurally disordered*, surface. Newer studies have been more definitive on this subject.^{110,111} The underpotential

oxidative deposition of nonmetals, such as iodine, at noble metals has also been studied. An example is shown in Figure 13, which depicts the potential-dependent structure and composition of Au(111) in dilute CsI.¹¹² The adlattice structures shown in this figure have recently been verified by *in-situ* STM.¹¹³

The first study of metal UPD at single-crystal electrode surfaces involved Ag on an *iodine-protected* Pt(111) electrode.¹¹⁴ The advent of ultraclean transfer conditions has allowed electrodeposition from solutions free of surface-active anions. Investigations, carried out in ClO₄⁻ or F⁻ electrolyte, include UPD of Cu on Pt(111);^{115–117} Tl, Pb, Bi, and Cu on Ag(111);¹¹⁸ and Pb on the three basal plane of Ag.¹¹⁹ The comparison, with respect to structural, catalytic, and electronic properties, of mixed-metal interfaces in both UHV and EC environments is a subject of current interest. A study that compared anodic stripping and thermal desorption of Cu at Ru(0001) found a remarkable similarity between the energy differences for the anodic stripping and thermal desorption of monolayer and multilayer Cu.¹²⁰

The controlled layer-by-layer growth, electrochemical atomic layer epitaxy (ECALE), of compound semiconductors by UPD has recently been reported.¹²¹ In the ECALE of CdTe, for example, one cycle would consist of the UPD of Cd followed by the UPD of Te onto the Cd monolayer deposit.

Molecular Adsorption Studies. UHV studies of water adsorption on single-crystal electrodes are based upon cryogenic adsorption.¹²² The structural and chemical properties of interfacial water are now well-documented. Of direct relevance to electrochemistry is the observation that, on Ni, Pt, Ag, Cu, and Pd, water is dissociatively chemisorbed, via hydrogen abstraction, if the surface contains *submonolayer* coverages of oxygen.

UHV-EC investigations of organic adsorption at single-crystal electrode surfaces, usually Pt, have been undertaken to understand the nature of the chemical interactions between the substrate and adsorbate as a function of interfacial parameters, such as pH and electrode potential, as well as to correlate the mode of attachment with the reversible and/or catalytic electrochemistry of these materials; molecular adsorption studies have been aided greatly by the recent addition of HREELS in the repertoire of surface analytical tools. Two studies with CO have been reported. One

sought to correlate anodic peak potentials with observed LEED structures at Pt(111);¹²³ the other examined the chemisorption of CO at well-defined and anodically disordered Pd(111).¹²⁴ Organic molecules, such as alkenes, homocyclic aromatic compounds, thiophenols, S-heterocyclics, N-heteroaromatics, and biologically-active molecules, have been studied.^{125,126} Mercapto compounds at Ag(111) were also investigated.¹²⁶

B. Electrolyte Characterization. Significant fundamental advances have been made during the past five years in characterizing the structure of the electrolyte at electrochemical interfaces. The necessity to consider the discreteness of solvent molecules and ions has been well established by experimental, computational, and theoretical methods during this time period. However, the significance of these molecular-level details in relation to equilibrium interfacial structures, such as underpotential deposition layers, and to electron-transfer dynamics has not yet been fully explored. The orientation and density of molecular films, the dispersion of semiconductor particles in photoelectrochemical cells, and the formation of ultrathin and stable wetting layers necessary for various forms of atmospheric corrosion are a few examples where molecular-level interactions between the electrolyte and the electrode are recognized as playing key roles. These structures are frequently discussed in terms of simple models of electrochemical double layers that are inferred from capacitance or surface tension measurements but which provide little direct evidence of molecular details. There are, in addition, many questions regarding electrolyte structure at metal electrodes that have yet to be explored by a direct experimental technique.

1. Experimental Measurements. The surface forces microbalance¹²⁷ (SFM) is an experimental system for measuring the nature and magnitude of interactions between two surfaces separated by a fluid medium. The basic measurement, recently developed¹²⁸ and now applied in many research laboratories,¹²⁹ consists of bringing two ultrasmooth surfaces (typically, but not limited to, molecular smoothness) together within distances comparable to the decay (Debye) length of the interaction being measured. Forces between the two surfaces are measured as a function of the distance separating the surfaces by means of optical and electromechanical measurements. Depending on the nature of the surface interactions, the measurements can be made over relatively large distances (10–1000 Å for electrostatic forces between two electrically charged or ionized surfaces) or short ranges (<30 Å for structural forces). More often, two or more types of surface forces with different decay lengths can be quantitatively measured in one experiment, resulting in a complete force law describing the surface interactions across the fluid.

The most fundamental and direct information about double-layer structure and ion adsorption has been obtained from surface forces microbalance measurements by investigators whose primary interests concern colloid chemistry. An example of the advanced stage of SFM measurements is the direct measurement of the thicknesses of Stern layers formed by adsorption of tetraalkylammonium cations on mica¹³⁰ (Figure 14). In these measurements, the distance of closest approach of the two surfaces (defined by an apparent hard wall contact) corresponds to twice the molecular diameter of the large organic cation adsorbed on the mica surface. The DLVO theory gives a good fit to the data beyond a separation distance of $2d$ assuming a plane of charge located at a distance d from each surface. The results are in excellent quantitative agreement with the Gouy–Chapman–Stern model.

Observations of solvent and ion layering (H_2O and organic solvents) between mica¹³¹ and metal¹³² surfaces are relatively recent and are not completely understood. These interactions cannot be described by a continuum fluid theory and have only recently been treated using physically realistic models of H_2O in computer simulations. The oscillations reflect the graininess of

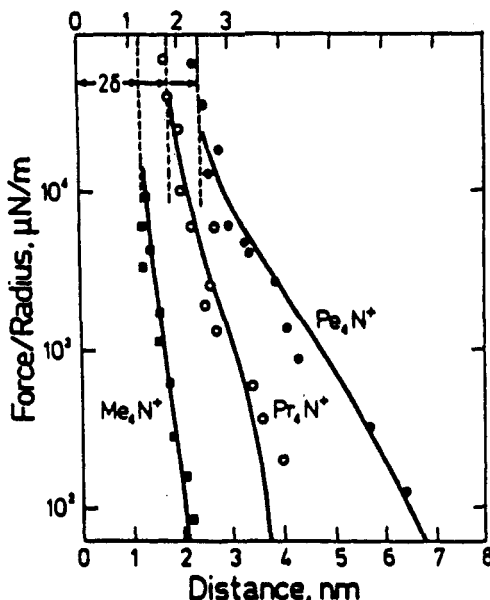


Figure 14. Forces between mica as a function of distance in concentrated aqueous solutions of $\text{R}_4\text{N}^+\text{Br}^-$ salts. $\text{Me} = \text{methyl}$, $\text{Pr} = \text{propyl}$, and $\text{Pe} = \text{pentyl}$.¹³⁰ The continuous curves assume a Stern layer of thickness d that corresponds roughly to the thickness of the adsorbed cation.

the liquid, and one expects that successful interpretation of electrochemical data may require consideration of the local interfacial structure, rather than the bulk properties of the liquid. In addition to oscillatory forces, a monotonically decaying repulsive or attractive structural force is often observed on hydrophilic and hydrophobic surfaces, respectively.¹³³ These forces are referred to in the literature as hydration and hydrophobic structural forces, and their origin is not completely resolved.

Surface-enhanced Raman spectroscopy (SERS) has been used with increasing frequency to probe interfacial solvent and ion distribution, primarily at a few metals (Au, Ag, and Cu) where the surface enhancement is largest.⁴ A number of recent articles have reported potential-dependent SERS spectra of H_2O and OH^- on Ag in aqueous solutions.¹³⁴ These studies demonstrate the feasibility of probing solvent molecules within the inner layer of the interface and those associated with the solvation shells of adsorbed cations. Progress has also been made in investigations of nonaqueous electrolytes. In principle, SERS is ideally suited to investigate intermolecular interactions (e.g., H-bonding) and metal–solvent interactions (e.g., dipole orientation) with high sensitivity and selectivity.

The measurement of X-ray reflectivity at an interface can provide the electron density profile normal to the interface. Thus, X-rays have potential as being very sensitive probes of the electrolyte structure, in addition to their use in characterizing surface reconstructions and roughness. The utility of the X-ray standing waves method, using synchrotron radiation, has been demonstrated as an *in-situ* technique to probe the potential-dependent distribution of iodide at the Pt–electrolyte interface.⁹³ Advances in this and related methods should provide a detailed fundamental structure of the solvent and ion distributions in the near future.

2. Theory and Simulations. Due to the complex physical structure of the double layer, theoretical investigations of electrolyte structure near a charged wall have largely focused on simplified models. Typical of these is the restricted primitive model in which electrolyte ions are represented by charged hard spheres (with embedded point charges) and the solvent is represented as a continuum dielectric.^{135–137} Beginning in the early 1980s, predictions of interfacial structures based on this and similar models have been obtained using integral equation methods and density functional theories. Inclusion of the finite ion size yields predictions of ion layering next to the surface and

charge inversion within the double layer, neither of which is obtained from previous statistical models employing point ion charges. These theories are quite successful in confirming Monte Carlo (MC) computer simulations of interfacial structures,¹³⁸ and extensions to more complex and realistic physical systems have been explored.¹³⁹

MC and molecular dynamics (MD) simulations of the electrochemical interfaces, beginning in 1980, have progressed to the level where it is now possible to model the molecular structure of an entire Pt/H₂O/Pt cell. Heinzinger and Spohr¹⁴⁰ have reported MD simulations of H₂O at Pt surfaces carried out using a Pt–H₂O interaction potential derived from extended Hückel orbital calculations. These results, as well as other MC/MD simulations,¹⁴¹ suggest that the dynamical properties of H₂O are affected by the surface only within the inner layer of adsorbed solvent molecules. Predictions of work function values and spectroscopic data gleaned from these investigations tend to be in semiquantitative agreement with experimental data, providing a direct test of the simulations. Other recent MD studies have focused on the dehydration and adsorption of ions at charged metal surfaces.¹⁴² It is very likely that continued progress in this area will provide details of solvent dynamics associated with heterogeneous electron transfer, following on initial investigations of model systems already carried out.¹⁴³

III. Interfacial Dynamics

A. Mechanisms and Elementary Processes. A great variety of dynamic events occur at electrode/electrolyte interfaces. Molecules and ions adsorb, atoms and molecules diffuse into and out of the interfacial region, surfaces reconstruct, ions and solvent molecules rearrange in the double layer, electrons transfer between the electrode and species in solution or bound to the interface, protons move among acid–base sites, ligands are lost or gained, leaving groups depart, radicals couple, and isomerizations occur. Mechanisms composed of individual, elementary steps produce complex and varied transformations. For example, the interfacial structure of a single crystal can evolve with time, so terraces enlarge and defects disappear. In another mechanism, water is produced by the addition of four electrons and four protons to molecular oxygen. In still another, a conducting material is formed by the electropolymerization of pyrrole, and this material can be switched electrolytically into an insulating state. A quite different type of mechanism is the basis for the measurement of glucose concentration by coupling of the enzyme glucose oxidase to an electrode via a mediating electron shuttle. By yet another set of elementary steps, one obtains an ordered fractional monolayer of copper on a single crystal of gold.

Mechanisms are studied to improve or thwart reactions, or to draw analogies for use in a different context. Methods for dissecting a mechanism into its elementary steps are as important in the study of electrochemical systems as they are in the study of homogeneous chemistry (in solutions or gases), but the interfacial case is more complicated, because one must reach beyond the inventory of homogeneous chemistry to include elementary processes involving the interface itself, i.e., *heterogeneous* steps such as interfacial electron transfer, adsorption, atom deposition, or reconstruction. Moreover, experimental approaches to mechanisms at interfaces are complicated by the quite small portion of an experimental system contained in the interfacial zone and the small numbers of species that are active there. Effective methods therefore must offer spatial selectivity and very high sensitivity.

Historically, our understanding of dynamics in electrochemical systems has been limited by the intrinsic complexity of the systems and by the lack of experimental tools with adequate sensitivity, range of time scale, or chemical specificity. New methodologies now allow fuller, more precise, and simpler studies of dynamics.

Ultramicroelectrodes and improved commercial electronics provide a basis for straightforward experiments with time

resolution on the microsecond and nanosecond time scales, where many elementary processes involved in electrode reactions are known to occur. Among them are protonation, isomerization, the ejection of leaving groups, and electron transfer. It is now possible to make direct observations of the kinetics of such processes; hence, the dissection of a mechanism becomes more direct and less dependent on models. Advanced methods for synthesizing interfacial structures, particularly by self-assembly, now provide access to simplified chemical systems whose dynamic characteristics can be examined in unprecedented detail. The study of heterogeneous electron transfer has especially benefited from this approach. The field still needs methods, however, that allow specific chemical moieties or surface structures to be monitored on a time-resolved basis.

One can explore some dynamic effects effectively by slowing molecular motions so that the measurements fall in a convenient time regime, e.g., by the application of high pressure and low temperature. Studies with electrolytes of extremely high viscosity (e.g., polymer films and transiently cross-linked polymer solutions) have shown that diffusion and other processes that depend on solvent motions (such as electron transfer) can be slowed by orders of magnitude in such media. The use of neither extraordinarily viscous media nor high pressure has been developed sufficiently to warrant further discussion here, but one can expect further developments. We discuss more fully in the following subsections advances in areas of particular importance.

B. Experimental Characterization of Heterogeneous Electron-Transfer Rates. This discussion focuses on progress in the measurement and characterization of the rates of heterogeneous electron transfer, i.e., the electron transfer between redox moieties and an electrode (metal, semiconductor). When the redox species are in solution, the standard heterogeneous rate constant is designated as k_s (cm/s). When the redox species are attached to an electrode surface, the standard rate constant is $k_{s,R}$ (s⁻¹); k_s or $k_{s,R}$ is the operative rate constant when $a_{ox} = a_{red}$ in solution or on the surface. The factors governing the rate of electron transfer are functions of the character of the electrode, the redox moieties, the electrolyte, and the intervening medium. Classical Marcus theory of electron transfer and derivative treatments predict a current–voltage relationship that significantly differs from the traditional Butler–Volmer relationship¹⁴⁴ when the driving force, $F(E - E^\circ)$, becomes comparable to, or larger than, the reorganizational energy, λ . A large driving force usually implies that the rate constant at an E significantly different from E° , k_E (cm/s) or $k_{R,E}$ (s⁻¹), will be very large at that applied potential and consequently difficult to measure. Characterizing rate constants over a large range of driving forces requires either the ability to measure very fast processes or strategies to slow down the processes in a controlled way (i.e., by decreasing the temperature).¹⁴⁵ Several new methodologies have evolved to measure, control, and characterize heterogeneous rate constants, i.e., methods utilizing microelectrodes, self-assembled monolayers, and laser perturbations.

1. Microelectrode Techniques. The typical microelectrode is a disk or a band. The critical dimension, r_0 , is the radius of the disk, (hemi)sphere, or (hemi)cylinder electrode or the half-width of the band electrode. Theoretical treatments of band and disk electrodes are complicated because current distribution over the electrode surface is not uniform under most electrochemical conditions.^{146–148} However, closely related to the band and disk electrodes are the hemicylinder and hemisphere electrodes that exhibit uniform current density and are described by much simpler theoretical treatments^{149,150} which often serve as adequate approximations for describing behavior at a band or disk. As discussed in section II.A.1, a decrease in the value of r_0 decreases the potential drop caused by uncompensated resistance, iR_u (where i is the current flowing in response to a potential perturbation and R_u is the portion of the resistance between the microelectrode

and the counter electrode that is sensed by the reference electrode), thereby facilitating faster changes in the interfacial potential. Although iR_u is not reduced to zero, positive feedback, a tricky electronic compensation (particularly if R_u is not constant), can effectively reduce it further.^{151,152} The present state of the art for relaxation methods at a microelectrode has effectively accessed the 10–100-ns time domain using potentiostatic^{153,154} or cyclic voltammetric methods,^{155,156} and values of $k_s < 10 \text{ cm/s}$ can be evaluated. A critical caveat might be noted: Virtually all chronoamperometric and cyclic voltammetric theory is based on the Butler–Volmer formalism. Deviation from Butler–Volmer behavior will occur when $F(E-E^\circ)$ is comparable to or greater than λ in a potentiostatic experiment or when

$$-RT/\alpha[0.78 + 1/2 \ln(\alpha FyD/RTk_s^2)] \geq \lambda \quad (3)$$

or

$$RT/\alpha[\ln(RTk_{s,R}/\alpha Fv)] \geq \lambda \quad (4)$$

in a cyclic voltammetric experiment.¹⁵⁷ An analysis of cyclic voltammetric behavior based on Marcus theory has recently been discussed.¹⁵⁸ A complete treatment which includes the appropriate Marcusian modifications of theory should be a straightforward task using simulation methods.^{159–163}

Progress in the measurement of these fast relaxations has depended upon development of effective instrumentation for measuring fast transients of small currents¹⁵¹ and elimination of stray capacitance in the electrode and electronics.¹⁶⁴ Measurement of $k_s > 10 \text{ cm/s}$ is inherently compromised by the diminishing quantity of material in solution that can diffuse to the electrode to react. Temporal separation of the capacitive current associated with charging the electrode double layer and the (usually) relatively smaller faradaic processes becomes increasingly important. Use of high concentrations of the redox species helps, but solubility and adsorption will present practical limits. When estimating the time constant for an electrode as $R_u C_{eff}$, C_{eff} , the effective electrode capacitance must include the faradaic component, which can be significant when the redox species are attached to the surface. For a small potential perturbation (<0.025 V) and a reversible electron transfer with a surface attached species:

$$C_{eff} = \text{area} \times C_{dl} + [F^2/RT(1/\Gamma_{ox} + 1/\Gamma_{red})] \quad (5)$$

The “faradaic” capacitance term for $\Gamma_{ox} = \Gamma_{red} = 10^{-10} \text{ mol/cm}^2$ would be $2 \times 10^{-4} \text{ F/cm}^2$, i.e., much larger than typical values of C_{dl} (the double-layer or film capacitance).

Quasi-spherical diffusion (to a disk) or quasi-cylindrical diffusion (to a band) enhances mass transport and diminishes diffusion control of heterogeneous electron transfer. Some impressively small electrodes ($r_0 < 10^{-6} \text{ cm}$) have been produced and characterized,^{57,165} and even smaller, but less well-characterized, electrodes have been fabricated.¹⁶⁶ Evaluation of k_s and α from steady-state measurements at ultramicroelectrodes, e.g., disks and hemispheres, has been described.^{167,168} The approach is based on the Butler–Volmer formalism, but incorporating Marcus theory should be possible. The accessible range of k_s is defined by the constraint

$$k_s r_0 / D \sim 10 \quad (6)$$

Thus, with a well-characterized electrode disk with $r_0 = 10^{-6} \text{ cm}$ and $D \sim 10^{-5} \text{ cm}^2/\text{s}$, a value of $k_s \leq 100 \text{ cm/s}$ might be measured.

Interesting questions are evolving about the meaning of electrochemistry at electrodes whose dimensions approach the molecular. Characterization of the geometry is difficult, and it becomes important to ask just how well the actual geometry is known before great effort is expended on detailed computations (e.g., the distinctions between the disk and hemisphere or band and cylinder may be moot). Several workers have discussed

deviations from “simple” diffusional control which can occur when the thicknesses of the diffusion layer and diffuse double layers become comparable at faster scan rates (or equivalently at smaller electrodes) and more dilute supporting electrolytes.^{169–171} The effect of redox species whose dimensions are comparable to r_0 , as well as the possibility of unique solvent structure near an electrode surface which manifests itself at electrodes with $r_0 < 10^{-6} \text{ cm}$, has also been considered.¹⁷²

Several variations of microelectrodes have been devised. A self-assembled monolayer with pinholes can act as an array of microelectrode disks.¹⁷³ With such an electrode, r_0 was about $(2-5) \times 10^{-7} \text{ cm}$, and values of k_s in the range 2–4 cm/s were deduced from impedance data. Another variation consisted of ubiquinone molecules dispersed in a virtually insulating self-assembled monolayer that acted as an array of microelectrodes, each with $r_0 \sim 10^{-7} \text{ cm}$.¹⁷⁴ An array of microelectrodes, as opposed to a single one, circumvents the problem of very small area and currents. Some interesting theoretical problems evolve as diffusion to an array progresses from behaving as a collection of individual disk electrodes with nonoverlapping diffusion layers (at short times) to a system with overlapping diffusion layers behaving as a planar electrode (at longer times).^{175,176}

An alternative approach involves the use of an ultramicroelectrode in an SECM (section II.A.1(a)), spaced a distance d ($d < r_0$) from a conductive substrate.^{177,178} In this case, the characteristic distance is d rather than r_0 and the heterogeneous reaction rates that can be measured are determined by the dimensionless parameter $k_s d / D$. The advantage of this approach is that the size parameter can be varied with a single ultramicroelectrode; larger, more easily fabricated electrodes can be employed, and the measured currents are enhanced by positive feedback from the substrate. Such an approach has recently been used to measure the k_s ferrocene oxidation in MeCN as 3.7 cm/s.¹⁷⁹

Summarizing, steady-state or relaxation measurements at microelectrodes can now access the equivalent of a 10-ns time domain and evaluate $k_{s,E} < \sim 5 \text{ cm/s}$. Improvements in fabrication and characterization of electrodes with r_0 approaching 10^{-7} cm could effect a steady-state measurement of $k_{s,E} = 1000 \text{ cm/s}$, eq 6. This would allow characterization of most heterogeneous electron-transfer reactions in the high-overpotential region. With improvements in the instrumentation for tracking the fast transients of small currents, the 100-ps time domain might be accessed, and measurements of $k_{r,E}$ or k (homogeneous first-order rate constant) = 10^{10} s^{-1} would be feasible.

Development of faster steady-state and relaxation measurements undoubtedly will reveal interesting information about heterogeneous rate processes. The techniques are not equivalent and may measure different reaction rates: e.g., for a system with adsorption which is potential dependent, where the adsorbed species are electroactive or electroinactive, or blocking or nonblocking (to electron transfer with solution redox species).

2. Surface-Attached Monolayers. The development of methods for producing self-assembled molecular monolayers which are covalently and virtually irreversibly attached to an electrode surface (see section IV) has led to a number of innovative studies characterizing heterogeneous electron transfer. For example, self-assembled monolayers of ω -hydroxyalkanethiols on gold electrodes have been produced, and the rate of electron transfer across these monolayers to a variety of redox couples in solution has been examined.^{180–182} Many of the parameters of electron transfer were examined in light of Marcus theory, including distance dependence (e.g., tunneling coefficient $\beta \sim 1$ per methylene unit of the attached thiol), reorganization energy, and the predicted limiting rate constant at large driving force. Conventional measurement techniques were applicable, since the rate of electron transfer was slowed by a factor of $\sim \exp[-\beta]$ for each methylene unit of the attached thiol. Defects that can act

as active sites, a critical problem with this approach,¹⁸³ were considered and were argued to be unimportant. An alternative approach involves the attachment (e.g., to gold electrodes) of self-assembled monolayers comprising mixtures of thiols with pendent redox groups and spacer thiols with no redox groups.^{161,184,185} This approach minimizes the possibility of electron transfer at active defects. The use of spacer thiols allows the surface concentration of the electroactive species to be varied while retaining the structure of a complete, self-assembled monolayer.^{161,185} The electron-transfer rate was slowed by an increase in the number of methylene units in the thiol, thereby positioning the redox centers further from the electrode surface. These slower rates were easily measured by conventional potentiostatic methods. Because $k_{s,r}$ is small, large overpotentials could be applied and a reorganizational energy for attached ferrocene moiety¹⁶¹ and a tunneling coefficient $\beta \sim 1$ per methylene unit of the thiol tether could be estimated.¹⁸⁴ Results for thiol-tethered $\text{pyRu}(\text{NH}_3)_6^{3+/2+}$ groups were similar,¹⁸⁵ suggesting either simple coincidence in the behavior of the two redox couples or alternatively that the alkane chain plays a dominant role in the electron transfer.

Measurement of the electron-transfer rates associated with surface-attached redox moieties cannot be measured using steady-state methods. As discussed in section III.B, relaxation methods work well and the amplitudes of the relaxations are enhanced because of the high concentration of reactive species positioned close to the electrode. A not inconsequential benefit of measurements involving self-assembled monolayers is that the often deleterious effects of adventitious adsorption are precluded.

The use of surface-attached monolayers has allowed the electrochemist to produce a well-defined surface structure in a relatively straightforward manner. The values of k_s or $k_{s,r}$ are often small enough (because of the distance between the electrode and the redox moieties) so that the effects of a wide range of overpotentials may be explored using conventional electrochemical techniques and macroelectrodes. Most of the work has focused on monolayers comprising aliphatic chains; varying the nature of the chains, e.g., using an aromatic or conjugated chain, should have a significant effect on the electron-transfer rate constants and the distance dependencies.

3. Open-Circuit Optical Perturbations and Pump-Probe Methods. Several authors have utilized pulsed laser heating to induce disequilibrium at the electrode/electrolyte interface and thus perturb the open-circuit potential; the relaxation of the open-circuit potential is a manifestation of dipole reorientation and charge transfer (electron or ion) across the interface. Approaches include direct laser heating of an electrode surface^{186,187} and indirect laser heating by irradiating the back (nonsolution) side of a thin-film electrode.¹⁸⁸ The latter approach has been used to measure values of $k_{s,r}$ as fast as 10^6 s^{-1} associated with electron transfer between a gold electrode and thiol-tethered ferrocene moieties.¹⁸⁴ The T-jump method avoids the problem of switching currents associated with the analogous coulostatic method and protecting the voltage amplifiers from overload¹⁸⁹ (problems that would be diminished at a microelectrode). A serious limitation is that only small perturbations are practical, and the large driving force domain is not easily accessed. (Large changes in interfacial temperature ($>5 \text{ K}$) would introduce a number of nonlinear effects which would greatly complicate analysis. Moreover, poising the system very far from the E° is not practical.) At the present stage of development, an $\sim 8\text{-ns}$ laser pulse effectively defines the short time limit. A faster laser, faster amplifiers, and faster data acquisition (all within the state of the art) could access the picosecond time domain.^{190,191} Reorganization energy could be deduced from the temperature dependence of $k_{s,r}$.

Any method that depends upon the direct measurement of electrical signals is inherently limited in its speed. The shortest time domains are accessed by methods which depend upon optical

perturbation and optical sensing (pump-probe). Several optical methods for sensing interfacial change (e.g., infrared¹⁹²), Raman scattering¹⁹³ or ellipsometry¹⁹⁴ coupled with a laser-induced temperature jump, offer the possibility of a pump-probe approach to study interfacial phenomena. The low sensitivity of these probes may require signal averaging. For example, the transient grating technique has been used to examine interfacial processes at semiconductors occurring in the low ps and fs time domains.^{195,196}

Methodologies are developing which can measure interfacial processes in the ps and fs time domains. Studies of redox species in solution will require increasingly high concentrations so that the following criterion is met:

$$1/[k_s(1/C_{\text{ox}}D_{\text{ox}}) + (1/C_{\text{red}}D_{\text{red}})] > 10^{-11} \text{ mol/cm}^2 \quad (7)$$

If $C_{\text{ox}} = C_{\text{red}} = 10^{-5} \text{ mol/cm}^3$ and $D_{\text{ox}} = D_{\text{red}} = 10^{-5} \text{ cm}^2/\text{s}$, then $k_s < 5 \text{ cm/s}$. Thus, no matter how small the accessible time domain, it is unlikely that $k_s > 10 \text{ cm/s}$ will be measurable. The very short time domains will be most useful for measuring electron-transfer rates associated with surface-attached species and for studies of relaxations of the interfacial region itself.

Since $iR_u = 0$ in an open-circuit method, electrode size is not critical, and fabrication and characterization of electrode surfaces are easier than for microelectrodes. A critical compromise, however, is that the time constant for the relaxation of the open-circuit potential affected by electron transfer is $R_{\text{et}}C_e$ where R_{et} is the electron-transfer resistance and C_e is the capacitance of the interfacial region. The open-circuit relaxation usually will be considerably faster than the potentiostatic relaxation for the same system.¹⁸⁴

Much remains to be done experimentally to learn to control and measure rates at a broad range of structured interfaces. On the conceptual level, the major outstanding issues involve the electronic coupling that drives electron delocalization. The dependence of the electronic coupling on the type of bonds linking the molecular site to the electrode is one particularly intriguing area that will be addressed in the future by systematic variations in linker chemistry. Another area is the dependence of the coupling on the electrode potential. In principle, the position of the Fermi level of the metal, which is determined by the electrode potential, should vary relative to the electronic levels of these linker bonds, and this variation should be important in determining the degree of electronic coupling through the linker. However, the evidence to date indicates very little potential dependence in the coupling.^{158,197} A wide range of experiments is needed to assess the generality of this result.

In parallel with good experiments, there is a clear need for accurate calculations of the electronic coupling and from that the rate of electron transfer. Quantum mechanical methods appropriate to these weakly coupled systems are being developed¹⁹⁸⁻²⁰⁴ and have been applied to some extent in cases of intramolecular electron transfer. In the case of transfer between an electrode and a molecular site, the first successful efforts may be *ab initio* calculations of the decay length of the coupling across simple linkers, even if accurate absolute rates are not yet accessible.

C. Interfacial Movement of Electrons and Ions. The electron-transfer concepts and experiments described above are essential to a full understanding of interfacial electron transfer. However, for many real situations, more complex situations must also be considered. In this subsection, we mention the kinds of effects that arise from coupling electron transfer to the motion of ions in the electrolyte or to other redox sites. As mentioned in the introduction to this section, chemical bond-making and -breaking processes are also often coupled to electron transfer; in section III.D we examine some aspects of these events in the context of catalysis at the electrode/electrolyte interface.

1. Electron Transfer in the Presence of Interfacial Charge. The presence of ionic charges on the electrolyte side of the interface is central to the energetics of the elementary electron-transfer

steps. The electron transfer is driven by the free energy change available to the electron as it moves between the electrode and a molecular site. The fraction of the total potential drop across the interface that is available to drive the electron transfer is determined by the distribution of the ionic charges. The Gouy-Chapman-Stern treatment²⁰⁵ of the electrostatics of the interface provides a continuum model for the distribution of mobile ions at the interface, and the Frumkin correction²⁰⁵ provides a way to incorporate the resulting potential profile into a treatment of electrode kinetics. These well-established approaches for simple interfaces must be adapted as we begin to examine molecularly structured interfaces where fixed ionic sites are often incorporated into the interface and where the redox sites can change the charge distribution to a significant extent as they undergo electron transfer. A treatment of such situations using continuum dielectric layers and continuous charge distributions has recently been presented.²⁰⁶ Experimental systems that allow their predictions to be confirmed are needed. Furthermore, because there have been only limited studies of the importance of treating the ions and solvent as discrete charges and dipoles, more work needs to be done with discrete electrostatic distributions at molecularly structured interfaces to see how accurately we will need to model these interfaces to understand fully their behavior.

2. Coupling of Electron Transfer and Ion Dynamics. The motion, as well as the position, of ions can couple to interfacial electron transfer. The best understood example is the macroscopic role that ion migration in the bulk electrolyte can have on the potential available at the interface at high current and at low supporting electrolyte concentration. With the advent of microelectrodes, it has been recognized that migration effects can be significant even at very low currents.¹⁷⁰ As we begin to consider electron transfer in smaller systems and at high intrinsic rates, we must account for ion motion as a coupled step in electron transfer. At the molecular level, ion motion, like solvent motion, will probably be best thought of as part of the outer-sphere reorganization needed to allow electron transfer to occur.

Finally, it is worth noting that with complex structures and films on electrodes we must consider the permeation of ions into the presumably densely-packed parts of the interface. This solid-state-like process may be very slow and may complicate the description of charge transport through the film. However, in cases where redox sites are embedded in the film, it may make a significant difference in the energetics of the electron-transfer reactions whether or not charge-compensating ions permeate the structure (see section IV.C.2).

3. Intermolecular Electron Transfer at Structured Interfaces. As molecularly structured interfaces become more fully understood, structures with multiple, distinct redox sites can be examined in detail. Such structures can mimic the kinds of behavior seen on longer length scales in electronically and redox conducting polymer film structures. For example, as has been done with polymer films,²⁰⁷ molecular diode structures might be assembled in which current flows easily from the electrode through one site to another but is restricted in the opposite direction by the thermodynamic barrier for electron transfer back through the first site; preliminary measurements have indicated the feasibility of such strategies using self-assembled monolayers.²⁰⁸ Moreover, molecular architectures that couple the electrode to catalytic sites via one or more intermediary sites will probably be constructed. Again such structures have analogs in similar structures assembled on a longer length scale using polymer films.²⁰⁹ To understand these new molecular assemblies in detail, we will need to consider electron transfer between molecular sites at the electrode/electrolyte interface. Issues such as the role of interfacial electric fields and the dielectric environments of the sites must be considered, as well as the requisite degree of coupling and the difference in formal potential between sites. Construction and measurement of the properties of such interfacial systems at

electrodes might also advance the understanding of other supramolecular structures, for instance, multiple site redox proteins in biological membranes, such as cytochrome *c* oxidase.

D. Catalysis. Electrode reactions are catalyzed when their rates are enhanced in the presence of an agent without consumption of that agent, just as in more conventional (thermal) chemistry. Understanding of electrocatalysis deserves a high priority, because it is essential to much of electrochemical technology (e.g., sensors, electrosynthesis, energy conversion, and storage), sometimes simply to elevate the rate of an otherwise slow process into a practical regime, sometimes to save energy, and sometimes to produce selectivity toward a particular electroactive species in a mixture or to promote the selective formation of a particular product among several possibilities.

All three purposes have parallels in applications of conventional homogeneous or heterogeneous catalysis, but energy savings appear differently in electrochemical systems than in thermal systems, where the saving comes from the ability to operate a process at lower temperature in the presence of the catalyst. Electrochemical processes can be activated in two ways, either by elevating the temperature or by using a larger electrical driving force (via application of a more extreme potential). The catalyst can reduce the need for activation in either respect. The product of the extra potential required for activation and the current at the electrode is wasted electrical power. By reducing the activation overpotential, the catalyst reduces the electric power consumption and the waste.

Electrocatalysis may arise from the electrode surface itself. Metals, alloys, and semiconductors often show specific catalysis of particular reactions, and they may be used readily as electrodes. They may also be dispersed on an inert conductor, such as high-area carbon, to produce a complex catalytic structure. Also, noncatalytic electrodes may be covered with catalytic films, as one finds with dimensionally stable anodes or catalytic UPD layers on metal supports.

A second general approach is to couple a known molecular catalyst, such as a transition metal complex or an enzyme, to an electrode. One can bind such a catalyst on the electrode surface in a monolayer or host it in a thicker film, perhaps in a polymeric matrix. One can also leave it free in solution, so that it acts literally as a homogeneous electrocatalyst. In all of these cases, there must be a means for transfer of charge between the electrode and the catalyst. Sometimes the catalyst offers this capability directly, but in other cases another redox agent must be employed to shuttle electrons between the principals. Significant progress has also been made by exploiting the natural selectivities of biological materials. The determination of blood glucose is an example of practical importance being one of several avenues for diabetic therapy. The early examples of ferrocene derivative/glucose oxidase catalysis of glucose oxidation have been recently extended to glucose oxidase (and other enzymes) to which donor/acceptor (D/A) mediators have been covalently linked or around which D/A-modified polymers have been electrostatically wrapped.²¹⁰ Enzyme-based electrocatalysis will be a continuing significant theme in improving the selectivity of the electrode/electrolyte interphase.

Activity in the first group of systems (catalytic surfaces) is rooted in the electronic properties of the active material, probably in the local electronic properties of "active sites", having configurations of atoms that are especially effective at the desired conversion, because they can form transitory bonds with the starting material or critical intermediates. This view is widely held because effective catalytic surfaces show performance that is highly dependent on the area of the surface and the manner of its preparation. Very smooth surfaces of single crystals are generally not very effective as catalysts.

On the other hand, the configuration of the active site is not known for any electrode process at any catalytic surface, so

mechanistic analysis is still at a very rudimentary level in these systems. Rapid progress on mechanism cannot be expected until ways can be found to examine the reactivity of specific sites of known structure. High return ought to come from the invention of means for synthesizing an array of identical sites on an electrode or even a single site on a microelectrode.

In section II, recent advances in the structural characterization of surfaces, including catalytic surfaces, are summarized. A good deal has been learned about the surfaces themselves and about the manner in which certain molecules bind to them. However, the data in hand relate almost entirely to static conditions. An effective catalyst requires rapid turnover at its active sites, and it may operate on intermediates rather than on starting materials. To gain structural insight into mechanistic aspects of catalysis at surfaces, one needs time-resolved structural information at atypical locations on the surface. This is a tall order, but progress can be expected in that direction. These considerations suggest that one cannot wisely base technological development entirely on the notion that better catalytic systems will arise rationally from an understanding of structure and mechanism. In the long run, perhaps, but the field is now quite far from the ability to pick out the relevant structure and events. In the short run, technological progress in systems based on catalytic electrodes inevitably depends on informed chemical intuition and exploration.

The situation is different for systems involving catalysts hosted at electrodes. In these cases, the active site is deliberately placed and has a known molecular structure, so the control of local architecture is much fuller than that for catalytic surfaces. Moreover, the hosted species are often selected on the basis of their known performance as homogeneous catalysts. Knowledge about their behavior can be obtained by studying their homogeneous chemistry with NMR or other means for examining dynamics with structural sensitivity. Thus, it is feasible to carry out mechanistic studies for systems based on hosted catalysts, and it is practical to work from the assumption that knowledge of structure and mechanism can lead to the designed improvements.

E. Structural Dynamics of Electrode Surfaces. The dynamic properties of the electrode/electrolyte interface are not confined to just the electrolyte and the molecular species at the interface; the electrode itself can be a dynamic material. The recent progress in structural characterization of electrodes with atomic resolution described in section II suggests the richness of dynamics we can expect at the atomic level. In addition to the local events that must accompany processes like underpotential deposition, surface reconstruction, or atom dissolution, we can see from the images now available with the scanning tunneling microscope that surface atoms must move tens and hundreds of angstroms in many electrochemical processes. Some STM studies have recorded the time dependence of structural change on the seconds and minutes time scales. The imaging of the formation, growth, and motion of pits one-atom deep during the dissolution of silver from silver-gold alloys²¹¹ or gold after etching with CN⁻²¹² are examples of the type of studies that can now be undertaken to track interfacial processes in time and space. This approach should lead to new insights into important technological processes, such as corrosion, electrodeposition, and alloy formation. We expect a dynamic, as well as atomistic, picture of these electrode processes to develop in the next few years.

IV. Chemical Materials and Microstructures

A. Introduction. This section outlines some recent advances in chemical materials and their organization at the electrode/electrolyte interface. In particular, an important theme in interfacial materials is the rational design of the chemical nature of the interfacial region. "Rational design" includes circumstances (i) where applying modern measurement approaches leads to a better structural or dynamic understanding of known kinds of

interphases and thereby of their electrochemical reactivity and (ii) when known chemical or electrochemical reactivities are used to fabricate a new interphase region possessing thereby a predictable structure or dynamic property. In the end, of course, these circumstances converge. The goals include a basic understanding of how to control electrochemical reaction kinetics, reaction pathways, ultimate electrosynthetic products, the selectivity of reactions conducted in the presence of multiple potential reactants, the robustness of an interphase to repeated or prolonged operation, and the sensitivity of electrochemical response applied as a chemical sensor.

Chemical materials comprising the designed electrode/electrolyte interphases can be categorized into three groups:

(a) The electrode surface presented to the electrolyte medium is a defined crystallographic plane or facet of an electronic conductor, e.g., a metal, a semiconductor, or an organic solid. Current research aims at an understanding of how the properties of the arrangement of surface atoms, and perhaps just as importantly of its nonidealities (e.g., step edges and other defects), affect the electrochemical reactivity of the interphase. This interfacial category (illustrated in Figure 1) offers a large challenge in atomic-scale understanding.

(b) Since the mid-1970s, considerable research has concentrated on how to attach molecular species (nonelectronic conductors) to electronically conductive electrodes (sometimes referred to as chemically modified electrodes).²¹³ The idea is to transfer the known chemical or electron-transfer reactivity of the attached molecular species to the electrode/electrolyte interface. These electrode coatings can contain either monomolecular or multimolecular layers of attached chemical sites. While the early monomolecular layers on modified electrodes were often structurally known, they were not coherently organized; most current monomolecular layer approaches attempt to introduce both structure and coherence (i.e., microstructure) into the electrode coating.

Electrode molecular coatings with multiple layers containing electronically discrete sites can also contain more than one kind of molecular site within the same coating, either randomly or spatially organized relative to one another and to the electrode, in a molecular microstructure. With these coatings, the traditional idea that the properties of electrode/electrolyte interfaces arises from layers of unimolecular dimensions becomes inappropriate. The electrochemical activity of multilayers of molecular materials on electrodes is more properly called an electrode/electrolyte interphase region, as depicted in Figure 1.

(c) The composition of an electrode/electrolyte interphase region is also affected by the molecular nature of the electrolyte medium, e.g., the "bulk" electrolyte. This material is traditionally considered as a solvent containing a dissolved ionic charge carrier component. Some new approaches of the composition of the solution side of the interphase region, e.g., novel electrolyte materials and especially those of low ionic conductivity, have been stimulated by the development of ultramicroelectrodes (see section II.A.1(a)).

B. Electrodes with Atomically Definable Interfaces. Electrodes with surfaces definable at the *nanometer* (e.g., atomic) level are of both fundamental and practical interest. Access to well-defined surfaces, as well as the ability to characterize and manipulate their structures, has been a vital component of fundamental studies of structure–property relationships in electrode processes. The foremost example of this is the use of single-crystal electrodes and the appropriate (atomic-level) methods to prepare and characterize their surface structures as discussed in section II. Atomically well-ordered metal surfaces can be prepared¹ by epitaxial growth in vacuum or as bulk single crystals whose surface single crystallinity can be attained by thermal annealing in UHV or under inert (ambient-pressure) gas. Epitaxial growth is

exemplified by the evaporation of Au to form smooth, ordered Au(111) films on cleaved mica surfaces.

One of the most important structure–property relationships for electrode surfaces is the relation of surface structure to electrode reaction rate in electrocatalysis. Many practical electrocatalytic surfaces are complex both in structure and composition, for example, electrocatalysts for CH₃OH oxidation that contain Pt added to other metals.²¹⁴ It is now possible to prepare, by a variety of deposition methods, multimetallic electrodes with tailored atomic arrangements of the different metals on the electrode. These surfaces are significant models for study of the mechanism of action of these practical fuel cell catalysts and of other catalytic surfaces that contain mixed metals in indeterminant chemical states. The goal is to attain a sufficiently detailed appreciation of how surface structure controls electrocatalytic reactivity, so as to be able to invert the experiment to fabricate a surface with optimal reactivity which can be translated into a practical catalyst (see section III.D).

A truly detailed description of an electrode–solution interface must include the atomic arrangement not only of the electrode surface but also of the ions, solvent, and other neutral molecules on the solution side of the interface. Such a detailed description might be said to be the “Holy Grail” of fundamental interfacial electrochemical studies of this interface and may not be attainable. One of the principal driving forces toward such a description is the advancement of theoretical models and computational approaches, most of which employ the tactic of segregating the interface into smaller sections that can be studied in great depth. This is at the heart of simulated double-layer experiments, as briefly described in section II.B.2. Although such theoretical studies¹⁴² are still in their infancy, an improved understanding of ion solvation in the inner Helmholtz layer is already emerging.

There are some studies, and opportunities for many more, of nonmetallic electrodes that have atomically defined and controlled interfaces. A wide range of single-crystal semiconductors (e.g., Si, GaAs, TiO₂) are available. In terms of well-defined and atomically flat surfaces, the layered semiconductors, such as WSe₂ and MoS₂, are of particular interest.^{215–217} The search for superconducting phases ensuing after the discovery of high-*T_c* perovskite–oxide superconductors has resulted in a profusion of new electronically conductive materials that could be employed in electrochemical systems. Many of these materials have high oxygen ion mobility²¹⁸ as well as electronic conductivity, properties attractive for electrode materials in high-temperature ceramic fuel cells and oxygen sensors. There is also interest in using high-*T_c* superconductor materials as electrodes at low temperatures, even at temperatures below the superconducting transition temperature, *T_c*. There is potential for fundamentally new electrochemical properties at an interface between a superconducting phase and a normal (electrolyte) phase. While interpretations are incomplete, changes in electrode reaction^{219–223} and double-layer²²⁴ parameters have been observed as temperature is lowered past *T_c*, and some theoretical investigations have been stimulated.^{225,226}

Electrococrystallization is another area where atomic-scale electrode surface definition is important. An example is the electrococrystallization of electronically conducting molecular crystals. Crystals of conductive donor (D)–acceptor (A) compounds, e.g., where D is tetrathiafulvalene (TTF) and A is tetracyanoquinodimethane (TCNQ), can be used as electrodes and can be modified electrochemically.²²⁷ Electrochemical approaches are also useful in growing crystals of D⁺A⁻ compounds.²²⁸ In a recent study, macroscopic single crystals of [D⁺–D⁺]^{[(TCNQ)_x]⁻ (where x = 2 or 4 and [D⁺–D⁺] = (*CpRu)₂(η⁶,η⁶-[2]₂)(1,4)cyclophane)²⁺) were formed electrochemically on Pt surfaces by reduction of TCNQ in electrolyte solutions containing [D⁺–D⁺].^{229,230} Depending on the applied current density, the resulting product is the purple salt}

[D⁺–D⁺]^{[(TCNQ)₂]²⁻ (an electrical insulator) or the black charge-transfer complex [D⁺–D⁺]^{[(TCNQ)₄]²⁻ (where σ(25 °C) = 0.2 Ω⁻¹ cm⁻¹). Electrococrystallization is also of interest²³¹ in ceramic processing including high-*T_c* materials, where electrochemistry may offer some new approaches to the fabrication of thin ceramic films of controlled composition and structure.}}

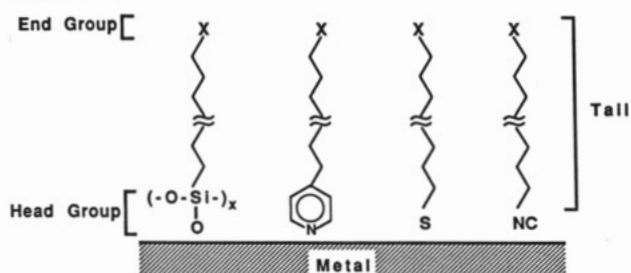
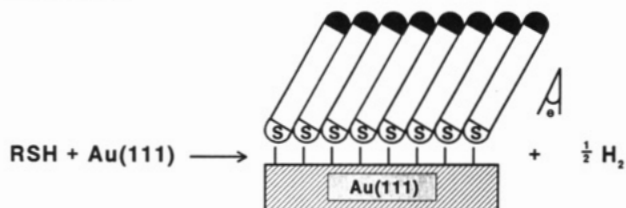
Multilayer structures are an important, relatively new class of materials in condensed matter physics and solid-state chemistry. The synthesis of such materials requires precise control of the growth conditions of each layer, especially at the interface between the layers. Examples are the high-Z/low-Z multilayers, such as W/C and Mo/Si used for X-ray lithography,²³² where atomically sharp interfaces are preferred over a compositionally mixed interfacial region. In magnetic multilayers with alternating layers of magnetic and nonmagnetic metals, it is not known how sharp the interface needs to be, but it is clear that nanometer-scale control of the layer thickness is required. A similar situation exists in semiconductor multilayer structures of interest in photovoltaic devices.²³³ Electrolytic processes may offer some advantages over the vapor deposition processes currently employed to fabricate multilayer structures. The ability to control independently the composition (via the potential) and the rate (via the current) makes electrolytic growth especially interesting for multilayer systems targeting atomically sharp interfaces, since electrodeposition can be conducted under conditions where both the substrate and deposited species are at ambient temperatures. Electrodeposition is a complex process, however, and methods to examine its progress at the atomic level have been developed only recently.²³⁴ There would appear to be an opportunity to exploit these new methods to probe electrochemical potentials for multilayer structure fabrication.

C. Molecularly Defined Electrode Surfaces and Novel Electrolyte Media. *1. Coherently Organized Molecular Structure at Electrodes.* Control of the molecular character of electrode surfaces has been attempted since the mid-1970s through attachment of chemical reagents to electrode surfaces. Chemical modifications aimed at predictably manipulating electrode responses²¹³ include a large number of schemes for immobilizing reagents on electrodes in monomolecular quantities and as thicker, multimolecular films made with polymeric materials and solid-state structures.^{235–238}

The earliest monomolecular layer immobilization schemes involved chemisorption and synthetic coupling of reagents to the electrode surface.²³⁵ The synthetic schemes relied on attaching electroactive reagents of interest (e.g., ferrocenes, porphyrins, quinones, viologens, metal complexes) to hydroxyl, carboxylate, acid chloride, and other functional groups on noble metal and on carbon electrodes. The redox and other chemical characteristics of such immobilized reagents are generally preserved,^{213,235–238} but limitations exist in stability and more particularly in an ability to define and control the structural and dynamic aspects of the immediate microscopic environment of the immobilized reagents. The recent themes²³⁹ of applying monomolecular layer films to electrodes by self-assembly and by Langmuir–Blodgett methods are beginning to address the latter. These themes and their promise for enhancing selectivity in electrode reactions are emphasized in the subsections that follow.

Electrode modification with multimolecular films of polymeric and other materials has offered improvements in stability of the electrochemical activity of the interphase region and in some aspects of control of the redox site environment. A substantial variety of materials now exist.^{213,235–238} Some recent work has focused on the transport of charge through these multilayer interphases, as discussed below.

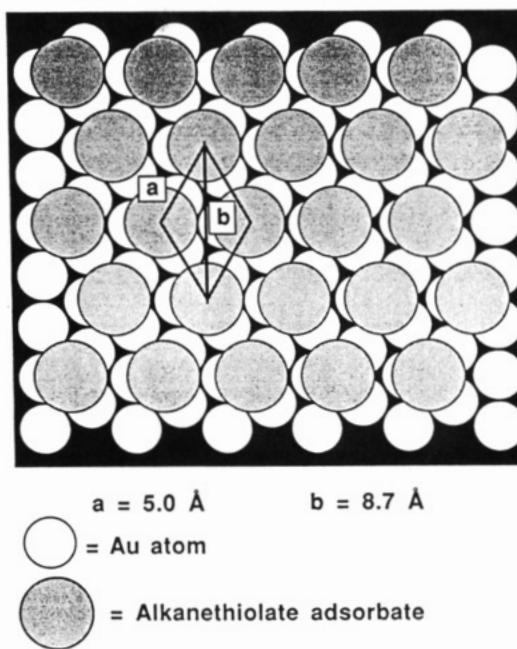
(a) Self-Assembled Monomolecular Films. Self-assembly of a molecular monolayer from a solution of a reagent onto a surface is generally a combination of two processes: binding of a chemical functionality on the reagent to the surface and a microstructural

SCHEME I**SCHEME II**

organization of the assembled monolayer that is driven by the hydrophobic effect and van der Waals attraction between low polarity (e.g., hydrocarbon-like) segments of the reagent. Examples (Scheme I) include silanes binding at hydroxylated surfaces,^{235,240} pyridine derivatives at platinum,²⁴¹ sulfur-containing compounds at gold^{240,242–247} and platinum,²⁴⁸ and isonitriles at platinum.²⁴⁹ Interest in such monolayers stems largely from their characteristic of good microstructural definition, which provides a needed platform for probing relationships between molecular microstructure on electrode surfaces and macroscopic electrochemical observables such as electrocatalytic potency and analysis selectivity. The control of molecular microstructure also allows research that addresses the limitations of predicting chemical and physical behavior at interfaces by extrapolation of bulk-phase properties. Importantly, the microstructural definition allowed by self-assembled monolayers has already provided fresh insights into electron-transfer reactions at electrodes^{161,197} and into other areas of interfacial science^{240,242,243} like adhesion, corrosion inhibition, friction and wear, and microelectronics.

General Structural Details of Gold Thiolates. Sulfur-containing compounds are strongly chemisorbed on gold surfaces and conveniently yield monomolecular films.^{240,242–247} Self-assembled monolayers formed from alkanethiols ($X(CH_2)_nSH$ with $n \geq 10$) seem to yield monolayers that are more densely packed and defect-free than do disulfide and sulfide precursors. The experimental details of forming these monolayers are important to their subsequent behavior. Key features are exposure time of the substrate to a dilute solution of the adsorbate precursor and the definition of the Au surface. The gold substrate is typically a 100–2000-nm film evaporated onto silicon, glass, or mica; polycrystalline gold has also been used.²⁵⁰ The most thoroughly characterized alkanethiol-type monolayers are those with $n \geq 10$ and small terminal groups (e.g., $X = CH_3, COOH, OH$). The results from macroscopic probes (e.g., infrared,^{245,251–253} X-ray photoelectron,²⁵⁴ and Raman spectroscopies,^{255,256} electrochemistry;²⁴⁵ and contact angles²⁴⁶) indicate that these alkanethiol monolayers have interfacial properties governed largely by X , are densely packed polymethylene chains tilted *ca.* 30° from the surface normal, and form as the corresponding thiolates. Microscopic structure studies support and expand on these findings. Diffraction^{257,258} and atomic scale scanning microscopic^{23,259} studies find a 0.5-nm nearest-neighbor separation distance for *n*-alkanethiolate monolayers, a spacing indicative of a ($\sqrt{3} \times \sqrt{3}$)-R30° adlayer at a Au(111) lattice.

Schemes II and III summarize these results, which are the beginning of a predictive structural model for such monolayers. Dominant considerations in the model are the large driving force

SCHEME III*

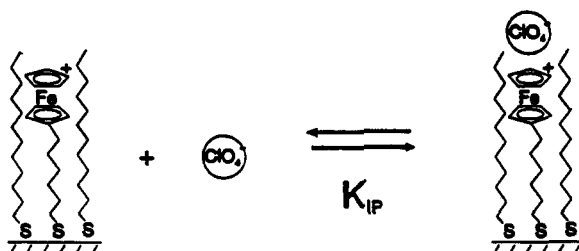
* From ref 43.

for gold thiolate formation (desorption activation energy *ca.* 30–40 kcal/mol²⁵¹) and the packing limitations imposed by the terminal group (X). Effectively, the energetics of thiolate chemisorption and the van der Waals attraction in the hydrophobic region yield a structure limited by the diameter of the chains of terminal X groups, thereby establishing the average tilt of the chains. For *n*-alkanethiolates on Au(111), the model predicts an average tilt of 27° that is in reasonable agreement with experiment. Thiolates with other small end groups (e.g., $X = OH, CO_2H$)^{251,252} and with a long perfluorocarbon tail^{252,260} also behave as predicted, as do (but not always as rigorously²⁶¹) those with bulkier end groups (e.g., ferrocenyl groups).

Other aspects of chemisorbed gold thiolate monolayers, however, remain poorly understood, leaving questions that complicate the design of specific interfacial architectures. Fabrication of mixed monolayers, containing more than one type of X, is an important step in manipulating local microstructure, but co-assembly experiments show²⁶² that the mole fractions of chemisorbed surface components do not reflect those of the solution reagents. A related issue is the macroscopic, two-dimensional distribution of the components of mixed monolayers: is the mixed monolayer phase segregated into small or large single-component domains,²⁶³ or are the components randomly mixed in two dimensions? Phase-segregated domains would not be surprising considering the behavior of some mixed Langmuir–Blodgett films. Recent laser desorption mass spectrometry²⁶⁴ results suggest that phase-segregated domains are smaller than about 30 μm, but defining a lower size limit has proved elusive.²⁶²

Barrier Properties. Gold thiolate monolayers are potentially useful barriers to mass or charge transport between the Au electrode substrate and the electrolyte solution. The aim is to shut off unwanted electrode processes, ultimately in a selective manner. Substantial effort has gone into assessing the presence of structural defects, e.g., pinholes of molecular size or larger, and how they are manifested in electrochemical behavior. Measurements of capacitance,^{173,245,252} electrolysis of solution redox species,^{173,245,252} underpotential metal deposition (UPD),²⁵² and gold electrooxidation^{173,265} reveal that barrier properties improve with longer polymethylene chains but insufficiently so for many of the targeted applications. The actual nature of monolayer defects^{245,263,266} is not altogether clear and may include atomic-level imperfections in the Au substrate surface (e.g., grain

SCHEME IV*



* From ref 272.

boundaries, step sites, and impurities) as well as the boundaries of monolayer domains (e.g., ordered domains tilted in different directions). An improved description of these monolayer defects awaits the development and application of suitable characterization methods, e.g., the coupling of scanning probe microscopies with terrain-altering reactions such as underpotential deposition or carefully controlled chemical etching.^{267,268}

Several defect-repairing or minimization strategies have been reported; most rely on filling defect pinholes with a second organic component. Self-assembled,^{161,173,269} electrodeposited polymeric,²⁷⁰ and functionalized silane²⁶⁹ films have met with varied degrees of success as fillers.

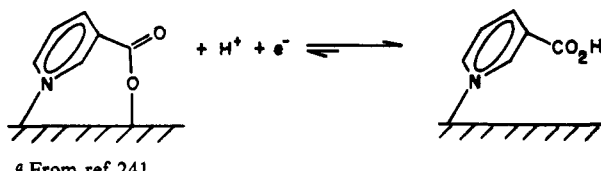
The use of monolayers as barriers to study the distance dependence of heterogeneous electron transfers was initially met with modest success even with electropolymerization-based pinhole filling²⁷⁰ (see section III.B.2). The first truly successful strategy to overcome leakage of electron charge through defects, and thereby confine electron transfer to tunneling through the alkanethiol barrier, utilized co-assembly of a ferrocene-terminated alkanethiol ($n = 15$) with an inert methyl-terminated alkanethiol ($n = 16$), followed by an exchange-annealing process.^{161,261} This procedure produced reasonably spatially isolated ferrocenyl^{161,261} and ruthenium pentamine¹⁹⁷ groups that appear to exhibit well-defined separation distance between the redox group and the electrode—key features for interfaces designed to test theories of electron transfer. Based on these important developments, exciting insights into electron-transfer processes should be forthcoming.

Manipulation of Reactions. A principal motivation in the microstructural organization of self-assembled films is control and manipulation of the microscopic environment of redox reactions. In one approach, co-assembled monolayers were fabricated from a mixture of electroactive and nonreactive alkanethiols.^{271,272} The alkane chain on one of the components was varied to alter systematically the immediate environment of the electroactive group (Scheme IV). Selected thiolate monolayers have also been used to manipulate charged surfactant²⁷³ and cytochrome c²⁷⁴ adsorption, observations potentially significant for study of electroanalytic selectivity and protein electron-transfer reactions.

Another aspect of ordered molecular monolayers is the nature of the electrical gradient imposed by the applied electrode potential. Gradients at bare electrodes can approach 10^6 V/cm over the first few layers of contacting electrolyte. For n -alkanethiolate monolayers, the total capacitance can be modeled reasonably well as a series of chemisorbed thiolate group and alkyl tail group capacitances. This model assumes that nearly all of the voltage is dropped across the monolayer and yields²⁴⁵ estimates of 3.5 and $50 \mu\text{F}/\text{cm}^2$ per carbon, respectively. Recent related efforts^{206,248,275} promise to place such findings on firmer experimental and theoretical grounds.

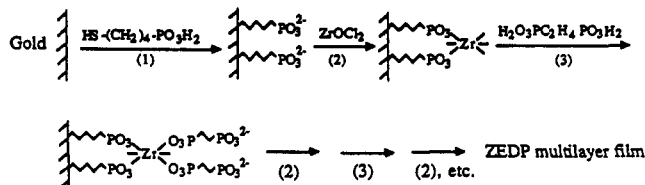
Design strategies for well-defined molecular interfaces need to consider other types of chemical transformations of chemisorbed monolayers as well. For example, self-assembled 3-pyridinecarboxylic acid monolayers²⁴¹ on Pt(111), adsorbed through Pt–nitrogen bonding with the aromatic ring tilted about 30° from

SCHEME V*



* From ref 241.

SCHEME VI*



* From ref 280.

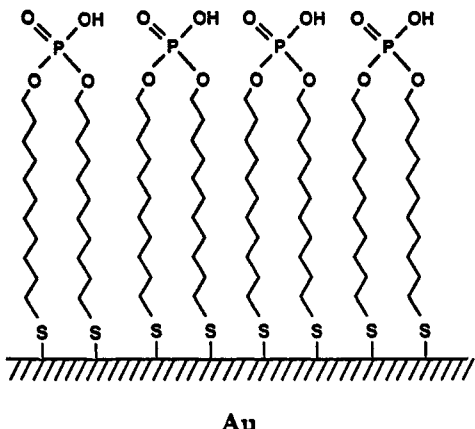
the surface normal, undergo an electrochemically-induced transformation upon application of a slightly oxidizing voltage. The conversion produces a nitrogen-tethered adsorbate that is also immobilized via chelation of the acidic moiety to Pt (Scheme V) and a substantial change in the chemical properties of the interface.

Self-Assembled Multimolecular Films. Self-assembly chemistry has also been employed to prepare multilayered structures, aimed at a more three-dimensional control of interfacial structure analogous to that sought via Langmuir–Blodgett deposition techniques. Approaches to date include sequential adsorption where either silane^{276–279} or thiol^{280,281} functionalities are used to tether the first layer to the substrate while chemical activation of an end group^{276–278} or electrostatic binding^{280,281} is used to bind subsequent layers. Scheme VI illustrates this with a multilayered structure based on a zirconium 1,2-ethanediylibis(phosphonate) (ZEDP) repeating unit. While the degree of microstructural ordering diminishes with increasing number of layers, these films are only beginning to be exploited as barrier films for electrochemical purposes,²⁸⁰ and they offer interesting prospects for devices exhibiting directional control of charge transfer and light propagation.

While a beginning framework exists for understanding gold thiolate and related chemisorbed monolayers, a truly molecular-level description of their associated structure–reactivity relationships will require experiments that probe their microstructural arrangement on a dynamic scale. The present descriptions largely reveal the average static interfacial structure, whereas events that govern electron transfer and ion motion at interfaces are strongly dynamic in nature. Approaches based on measurements at greatly reduced temperature²⁸² and at extremely short electrolysis times¹⁵⁴ could be possible first steps to this end.

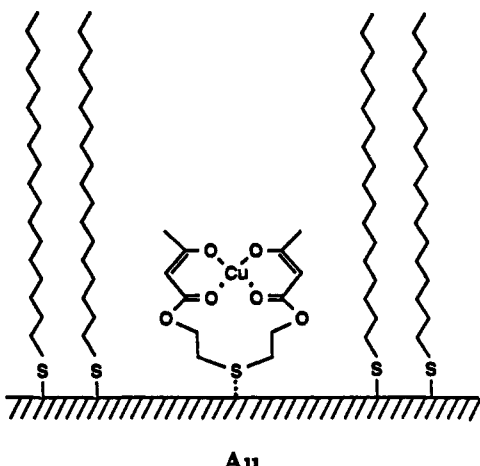
Microstructural manipulation of molecular interfaces should also benefit from an expanded repertoire of preparative techniques. Groups such as SeH²⁸³ and PH₃²⁸⁴ that also bind to gold have not yet been extensively characterized, and additional immobilization chemistries will probably be invented as the research in this area progresses. Thiol-based monolayers on semiconductor surfaces, such as GaAs,²⁸⁵ have recently been developed, opening opportunities in photoelectrochemistry. Oligoimide monolayers constructed at Au through thiolate linkages,²⁸⁶ variation in head group structure,^{287–290} and two-dimensional patterning of monolayers²⁹¹ should in time lead to development of many interesting new materials.

(b) **Selectivity in Electrode Reactions.** Selective response and a desire to introduce elements of molecular recognition in electrode reactions are major goals in electro-organic synthesis^{292,293} and in the design of selective electrochemical sensors.²⁹⁴ Chiral induction in electrosynthetic reactions is a particularly challenging issue. Early chiral induction strategies relied on chiral solvents, chiral supporting electrolytes, and chiral adsorbates.²⁹³ Subse-



Au

Figure 15. Schematic structure of a self-assembled monolayer of a dithiol derivative of diundecyl phosphate which exhibited pH-dependent ion-gating properties with respect to ferricyanide ions.²⁹⁹



Au

Figure 16. Schematic structure of a self-assembled monolayer consisting of octadecylthiol and 2,2'-thiobis(ethylacetoacetate) (TBEA). The enol form of TBEA selectively complexes cupric ions in the presence of ferric ions, thus inducing selective response of the modified electrode. Reprinted with permission from *Nature*, ref 271. Copyright 1988 Macmillan Magazines Limited.

quently, Miller and co-workers²⁹⁵ introduced the idea of coupling a chiral reagent (e.g., (*S*)-(−)-phenylalanine methyl ester) to a carbon electrode surface to create a chiral environment at the electrode/electrolyte interface. This experiment produced a small enantiomeric excess of the chiral 4-acetylpyridine reduction product. Later investigations described reactions at electrodes modified with poly-L-valine,²⁹⁶ cyclodextrin films,²⁹⁷ and sodium montmorillonite clay layers.²⁹⁸ Generally, however, limitations in controlling the detailed microstructural environment of the electrode reactions have hampered a thorough mechanistic understanding of these selectivity effects.

Ion-selective and ion-responsive molecular films on electrodes are another form of molecular assembly aimed at induced electrode reaction selectivity. Their functioning for a self-assembled monolayer film is illustrated²⁹⁹ in Figure 15. The ordered monolayer of the diundecylphosphate dithiol derivative is ion-gating, in an electrolyte pH dependent manner. Specifically, ferricyanide reduction is blocked at pH > 4, where the phosphate groups of the monolayer assembly are partially or completely ionized, whereas permeation of ferricyanide through the monolayer and reduction is largely unimpeded at lower pH values. Analogous electrostatic effects have been observed in other self-assembled thiol derivatives on gold electrodes³⁰⁰ and in multilayer assemblies³⁰¹ of phospholipid molecules containing anion- or cation-binding species such as lipophilic macrocyclic polyamines and valinomycin. Binding of "guest" anions or cations by the

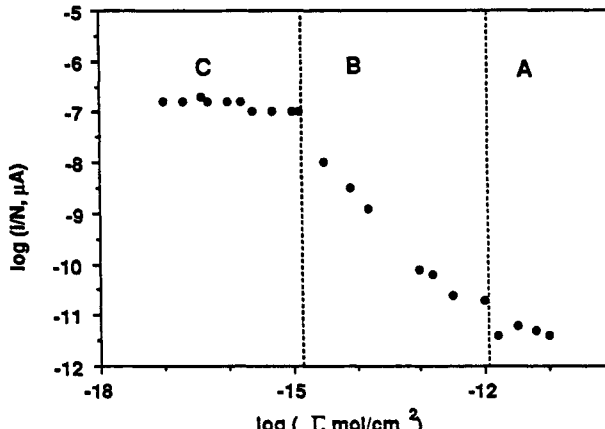
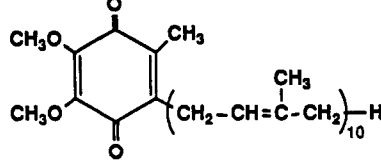


Figure 17. Plot of $\text{Ru}(\text{NH}_3)_6^{3+}$ limiting reduction current per ubiquinone (Q_{10}) site (inset shows the structure of Q_{10}) vs ubiquinone surface concentration. Q_{10} molecules are incorporated in a $\text{C}_{18}\text{SH}/\text{C}_{18}\text{OH}$ L-B monolayer on gold electrode. The increase in i/N reflects mass-transport enhancement due to radial diffusion which dominates transport of $\text{Ru}(\text{NH}_3)_6^{3+}$ with decreasing surface concentration of Q_{10} sites in the monolayer assembly. It is postulated that the isoprenoid chain of ubiquinone forms a channel in the otherwise impermeable L-B monolayer which allows access of $\text{Ru}(\text{NH}_3)_6^{3+}$ to the electrode surface. From ref 305.

latter film constituents induces changes in permeability of the films to charged electroactive probe species.

A more sophisticated ion-selective monolayer assembly,^{271,272} consisting of 2,2'-thiobis(ethylacetoacetate) (TBEA) and *n*-octadecyl mercaptan co-self-assembled on a gold electrode, is shown in Figure 16. The impermeable octadecanethiol monolayers constrained electroactivity in this system to the TBEA sites, which being more specific to Cu^{2+} coordination led to its selective electroreduction in the presence of ferric ions. An analogous self-assembly scheme³⁰² immobilized a quinone derivative in an alkanethiol monolayer for the electrocatalytic oxidation of NADH.

Self-assembled films have two limitations with respect to producing two-component monolayers, namely (a) thiol and disulfide derivatives of the components are needed for self-assembly on gold and silver surfaces²³⁹ and (b) a better control would be desirable for the concentration of the active sites of molecules in the surface monolayer. Langmuir-Blodgett (L-B) transfer techniques offer some relief from these limitations and constitute an alternative strategy for preparation of ordered monolayer assemblies at electrodes. L-B films also have a wide range of applications with a correspondingly well-developed chemistry.^{239,240,303}

Precise control of the (average) composition of multicomponent monolayer assemblies is readily achieved in L-B transfers in which the monolayer components are initially spread at the air/water interface and then compressed and transferred to the electrode surface. Control of the surface density of active sites incorporated in an otherwise passivating monolayer is illustrated in Figure 17 for a monomolecular L-B assembly^{304,305} containing octadecanethiol (C_{18}SH) and octadecanol (C_{18}OH) as components responsible for electrode passivation; ubiquinone (Q_{10}) defines sites of electroactivity. The surface concentration of ubiquinone in the $\text{C}_{18}\text{SH}/\text{C}_{18}\text{OH}$ monolayer was varied from 10^{-11} mol/cm² (ca. 10% of the monolayer structure) to 10^{-17} mol/cm² (where the average spacing between individual Q_{10} sites is ca. 1 μm). The

dependence of the reduction current for $\text{Ru}(\text{NH}_3)_6^{3+}$ calculated per Q_{10} site, $i/N(\text{Q}_{10})$ (the vertical axis), on surface concentration shows that at a sufficient dilution the Q_{10} molecules act as individual active sites.³⁰⁵ That is, the ubiquinone molecules function as single-molecule "gate" sites that open access to the electrode surface through an otherwise impermeable $\text{C}_{18}\text{SH}/\text{C}_{18}\text{OH}$ L-B monolayer. Systems like this are potential models of ion channels in phospholipid membranes. In related work, permeability of phospholipid monolayers containing gramicidin and other peptide ionophores on mercury electrodes has been investigated recently.^{306,307}

The above $\text{C}_{18}\text{SH}/\text{C}_{18}\text{OH}/\text{Q}_{10}$ L-B monolayer system is an organized assembly designed for two specific functions: *passivation* and *gating*. Constraining the heterogeneous electron transfers of species in solution to the gate sites offers novel opportunities to control the chemical microenvironment of the reaction, e.g., to induce elements of "selective gating" based on such molecular characteristics of gate *vs* solution species as size, shape, charge, and chirality. Electrochemical currents are typically interpreted in macroscopic terms; this strategy suggests possibilities for interpreting currents in terms of multiples of microscopic electron-transfer events at a known number of molecularly well defined sites. At the same time, other new interpretive issues present themselves for surface monolayer active site concentrations below *ca.* 10^{-15} mol/cm² (see Figure 17). In an array of independent molecular sized ultramicroelectrodes, the diffusion layer and the electrical double layer may have similar dimensions, leading to migration effects and distortions in the mass transport flux and the position of voltammetric waves.¹⁷⁰ These factors will require consideration in interpretation of current-voltage curves for determination of heterogeneous rate constants.

Self-assembled and L-B monolayers are also attractive as organized platforms for immobilization of enzymes on electrodes. For example, glucose oxidase has been immobilized in a phospholipid L-B monolayer³⁰⁸ and transferred to an electrode as a single-component L-B multilayer assembly,³⁰⁹ and self-assembled bilayer structures have been reported.^{310,311} The bilayer assemblies constitute both a medium for enzyme immobilization and a means for electron transport between enzyme and the electrode via lateral diffusion of the electroactive amphiphiles along the bilayer assembly. In areas other than electrochemistry, specific protein-lipid interactions have been of interest,³¹² and the catalytic activity of cholesterol oxidase was evaluated directly at the air/water interface.³¹³ Binding of monoclonal antibodies to supported phospholipid monolayers³¹⁴ has been investigated. These latter investigations suggest possibilities for new ordered monolayer and multilayer electrode structures of previously unmatched selectivity, specificity, and range of application.

2. Environmental Dynamics. It is now recognized that many aspects of electrochemical behavior involve not only the dynamic characteristics of the electron transfer donor (D) and acceptor (A) reaction participants but also the chemical environment around the D/A electron-transferring species. This subsection describes the relation between electrode reactant/electrolyte interphase dynamics for interphases more amorphous than those in the preceding subsection. This discussion is organized by the intended characteristic of the D/A environment, e.g., the dipolar relaxation properties of the electron-transfer donor or acceptor's solvent shell ("solvent dynamics"), the relation of physical mobility of a D/A moiety spatially affixed within the interphase region to the delivery of charge to the electrode, and the temperature of the surrounding medium.

(a) Solvent Dynamics. Investigation of the energetic role of the solvent shell surrounding a D/A reactant pair is a long-standing theme in electrochemical and homogeneous solution investigations of so-called outer-sphere electron-transfer kinetics. Modifications of the highly successful theory³¹⁵⁻³¹⁷ accounting for solvent

energetics, to include the role of dynamics of solvent dipolar reorientations³¹⁸ in achieving the isoenergetic state through which D passes to A, have restimulated experimental activity in electron-transfer measurements, including those at electrode surfaces.³¹⁹ The preponderance of evidence has established the importance of the solvent dipole relaxation rate, as embodied in the longitudinal relaxation time τ_L . The most convincing experimental approaches have involved measurements of heterogeneous electron-transfer rate constants³¹⁹ for outer-sphere D/A reaction pairs obtained in a series of solvents of known τ_L . Important solvent species are acetonitrile, CH_2Cl_2 , pyridine, DMSO, and propylene carbonate, with τ_L values ranging from 0.2 to 2.5 ps.

While theoretical progress will surely continue, the boundaries of solvent dynamics electron-transfer rate control can be further explored by choosing solvent environments in which the dipolar relaxation time constant can be systematically manipulated. The addition of sucrose to water³²⁰ and the use of polyether solvents^{321,322} of varied chain length and containing varied supporting electrolyte concentration have produced systematic changes in heterogeneous electron-transfer rates, showing the fruitfulness of this approach. Its difficulty is the greater molecular complexity of the solvent environment and a lack of a priori knowledge of the value of τ_L .

While such measurements have not yet been reported, electron-transfer kinetics of electrode-attached monolayers of D/A as a function of the solvent employed can now be studied. These experiments would be based on the use of microelectrodes,⁵⁶ as discussed in section II, and would require choices of suitably adiabatic electrode-attached D/A pairs.³¹⁹ This type of electrode kinetics would also probe the relation between monolayer-modified electrode interface structure and the local electrolyte solvent structure and dynamics.

(b) Dynamics of Donor/Acceptor Sites within Electroactive Polymer Films on Electrodes. These chemical systems^{213,235-238} involve various D/A sites covalently attached to (or comprising) a polymer network or "electrostatically bound" as the counterions of a polymer having fixed ionic sites, within polymer films of thicknesses from a few nanometers to a few microns. Electrons are delivered to the D/A sites by a site-to-site hopping process which for electrostatically bound reactants is coupled to their diffusion. Studies of the polymer film interphase region have been extensively driven by interests that include the electrocatalytic reactivity of polymer film sites,³²³ electroanalysis using sites as reagents,²³⁸ and understanding the chemical and physical aspects of the electron-hopping chemistry itself.³²⁴ While understanding of electron hopping (e.g., self-exchange) in the polymer films has advanced since investigations started in the 1980s, numerous issues remain unresolved, and new ones have arisen.³²⁵

A major issue is uncertainty in both structure and dynamics of the molecular environment of the electron-transfer events that occur between electron donor and acceptor states within the polymer phase. The polymer generally contains monomer solvent imbibed from the contacting (monomer) solvent/electrolyte solution; the amount and role of this solvent are generally unknown, as is whether its energetics and dynamics (e.g., τ_L) are changed in the polymer (i.e., what constitutes the "solvent" for the D/A pair?). Our understanding of the dependencies of electron-hopping rates on "fixed" D/A site concentration is incomplete and requires consideration of the degree of thermal and electrostatically driven oscillation of the site around its equilibrium position,³²⁶ the site-site distance dependence of electron hopping,³²⁷ and what interactions between the D/A site and the surrounding polymer and/or ionic species occur and affect the electron-transfer activation barrier.^{328,329} Valuable additions to these studies would be further model chemical materials with dynamic properties that are readily measurable with ancillary methods and can be systematically manipulated. Another route

to an improved understanding of environmental dynamics in the interphase region may exploit liquid crystalline materials, for which some studies have already appeared.³³⁰

Another major issue in polymer interphase electron transfers is the interplay between the mobilities of the electron, of the D/A sites, and of ionic components of the polymer. This has provided a level of complexity only recently appreciated.^{328,329} Electron-ion coupling occurs, and electrical gradients arising from low mobility of ionic species in the polymer facilitate electron-hopping rates. This issue raises the need for electroactive polymer materials for which relative values of these three mobilities can be independently known or measured. D/A site mobility, for example, should be a function of polymer cross-linking and of ion-ion site interactions; ion mobility should be a function of ion solvation. Low ion mobility can be achieved by lowering temperature, lowering the solvent content of the polymer film, or using a polymeric counterion, and in the limit the effects of the electrical gradient dominate the electron-hopping kinetics.³³¹⁻³³⁴

Other new types of film-coated electrode studies pertain to metal/solid insulator interfaces. Ultramicroelectrode tips and very thin layers of solid insulators can be used in SECM or STM experiments to study charge injection at the metal tip/insulator interface. For example, scanning tunneling spectroscopy of the Pt/TiO₂ system has produced information about the location of the energy bands and surface states.^{51,52} Similar studies of organic insulator films and photoconductors should be possible. By investigation of the injection current-potential behavior, the energies of filled and vacant orbitals, of traps, and of surface states and the density of state distributions should be accessible; two-dimensional surface scans could then yield the distribution of states on the surface. Such studies should be of interest in imaging systems (electrophotography), molecular material-based electronic devices, and solar cells.

(c) *Temperature.* Relatively few electrode/electrolyte interfacial dynamics studies have relied on manipulation of temperature, in spite of the well-known advantages of thermal control of reaction rates including the mechanistic diagnoses possible by differential quenching in multistep processes and the importance of thermally derived activation parameters. Historically, lowered electrolyte solution temperatures have not been popular owing to the accompanying diminished ionic conductivities, but microelectrode methodology has made quantitative work possible even in resistive media like toluene and hexane.^{335,336} A chemical materials problem is the development of well-characterized cryogenic solvent-electrolyte systems to complement existing ones like butyronitrile,^{337,338} which is useful to 138 K, and butyronitrile/ethyl chloride mixtures,³³⁵⁻³³⁸ which have been used at 88 K but which are more generally accessible to *ca.* 105 K.

In the other direction, elevated temperatures are important in promoting electrode reaction rates in aqueous-acid fuel cell media, but fundamental electrode/electrolyte interface work on other reaction types or solvents has been quite limited in scope. Electrochemist's favorite solvents, acetonitrile and methylene chloride, are quite volatile, but there may be reluctance to explore different solvent media. Polyether polymer electrolytes³³⁹⁻³⁴⁵ have the thermal stability and nonvolatility needed, as an example. Another approach is to employ both high temperature and high pressure, e.g., in studies in near-critical and supercritical fluids.⁵⁴ Elevated temperatures should be a powerful tool for dynamics studies of slow electron transfer and associated chemical events.

V. Conclusions

The field of electrochemistry necessarily comprises a rich assortment of subdisciplines addressing problems relating to structure, dynamics, and material properties of the interfacial region and its components. New methods for *in-situ* characterization have been evolving over the last decade, and these are providing the main methodological driving force for new inves-

tigations of the electrode/electrolyte interface identified in this report. The *in-situ* (as opposed to *ex-situ*) methods permit characterization of the interfacial region in solution under reaction conditions. X-ray scattering methods (whose evolution paralleled the construction of synchrotron light sources) and scanning probe microscopic methods can reveal the structural status of the interfacial region while an electrochemical reaction is proceeding. Variations of Raman and infrared techniques can effect *in-situ* identification of adsorbates which may be reactants, products, or intermediates in an electrochemical reaction. The surface forces microbalance has given some new insights into the nature of the electrolyte structure within angstroms of an electrode surface. The age-old problem of correlating the microscopic structure of the interfacial region and the electrochemical function of an electrode can now be meaningfully addressed, but it is clear that the requisite theory has yet to be developed. The new methodologies also offer the possibility of time-resolved structural analysis. The scanning tunneling microscopic methods may well be able to capture information in the millisecond time domain, and more powerful synchrotron light sources (which are pulsed) may well be able to probe structural changes occurring on the microsecond and submicrosecond time scale.

Studies of interfacial dynamics were also deemed critical for understanding the behavior of the electrode/electrolyte interface. Our ability to access increasingly shorter time scales for studies of interfacial dynamics has made great progress but continues to lag behind studies of homogeneous dynamics which now routinely access the picosecond and even the femtosecond time domains. Ultramicroelectrodes have proved to be powerful tools which can query processes occurring in the submicrosecond time domain. Novel optical perturbations, improved electronics and data acquisition, and the development of lasers with shorter, more powerful pulses may well be able to probe interfacial dynamics in the subnanosecond time domain. The use of a self-assembled monolayer to control the distance between an electrode and redox moieties (attached or in the electrolyte), as well as to control the properties of the intervening medium, has led to an improved understanding of the fundamentals of heterogeneous electron transfer. An important facet of this approach to modifying and controlling interfacial structure is the possibility of producing interfacial films with selective electron, ion, and molecular transport properties which can act as the basis of sensor systems. Fundamental studies like these will also be useful in many other applied areas. These include electrosynthesis; electrocatalysis; characterization of materials; analysis and characterization of solution composition, structure, chemistry, and dynamics; and energy storage and conversion.

Acknowledgment. We appreciate the assistance of Peter Flynn, Peter Rossky, and Phil Ross in the preparation of this report. The support of the Department of Energy, Council on Materials Sciences, is gratefully acknowledged.

Editor's Comment. This feature article is different from other feature articles we have published. However, in a field as rapidly developing as the one discussed in this article, it is useful for scientists in the field if such an article is published in this section. It is a combined and a fruitful effort of several active scientists in the area, and I feel it will have the impact of several feature articles. This paper is also a summary and a critical evaluation of the present and future status of the field. For this reason, the length restriction was relaxed.

References and Notes

- (1) Soriaga, M. P. *Prog. Surf. Sci.* 1992, 39, 325.
- (2) Bewick, A.; Kunimatsu, K.; Pons, B. S. *Electrochim. Acta* 1980, 25, 465.
- (3) Stole, S.; Popenoe, D.; Porter, M. In *Electrochemical Interfaces, Modern Techniques for In-Situ Interface Characterization*; Abruna, H., Ed.; VCH Verlag Chemical: Berlin, 1991; p 399.

- (4) Pemberton, J. In *Electrochemical Interfaces, Modern Techniques for In-Situ Interface Characterization*; Abrufa, H., Ed.; VCH Verlag Chemical: Berlin, 1991; p 193.
- (5) Perry, S.; Campion, A. *J. Electron Spectrosc. Relat. Phenom.* 1990, 45, 933.
- (6) Ansermet, J. P.; Slichter, C. P.; Sinfelt, J. H. *Prog. Nucl. Magn. Reson. Spectrosc.* 1990, 22, 401.
- (7) Chan, K. W. H.; Wieckowski, A. *J. Electrochem. Soc.* 1990, 137, 367.
- (8) Slezak, P.; Wieckowski, A. *J. Electroanal. Chem.* 1992, 339, 401.
- (9) Wieckowski, A. In *Modern Aspects of Electrochemistry*, Vol. 21; Bockris, J. O'M., Conway, B. E., White, R. E., Eds.; Plenum: New York, 1990; p 65.
- (10) Krauskopf, E. K.; Wieckowski, A. In *Frontiers of Electrochemistry*; Ross, P. N., Lipkowski, J., Eds.; VCH Verlag Chemical: New York, 1992; p 119.
- (11) Buttry, D. A. In *Electroanalytical Chemistry*, Vol. 17; A. J. Bard, Ed.; Marcel Dekker: New York, 1991; p 1.
- (12) Bonnenfeld, R.; Hansma, P. K. *Science* 1986, 232, 211.
- (13) Liu, H.-Y.; Fan, F.-R. F.; Lin, C. W.; Bard, A. J. *J. Am. Chem. Soc.* 1986, 108, 3838.
- (14) Sonnenfeld, R.; Schardt, B. C. *Phys. Lett.* 1986, 49, 1172.
- (15) Cataldi, T. R. I.; Blackham, I. G.; Briggs, G. A. D.; Pethica, J. B.; Hill, H. A. O. *J. Electroanal. Chem.* 1990, 290, 1.
- (16) Snyder, S. R.; White, H. S. *Anal. Chem.* 1992, 64, 116R.
- (17) Oudar, J.; Marcus, P.; Clavilier, J. *J. Chim. Phys.* 1991, 88, 1247.
- (18) Wiechers, J.; Twomey, T.; Kolb, D. M.; Behm, R. J. *J. Electroanal. Chem.* 1988, 248, 451.
- (19) Itaya, K.; Sugawara, S.; Sashikata, K.; Furuya, N. *J. Vac. Sci. Technol. A* 1990, 8, 515.
- (20) Clavilier, J.; Nodes, A.; Achi, K. E.; Zamakhchari, M. A. *J. Chim. Phys.* 1991, 88, 1291.
- (21) Gao, X.; Hamelin, A.; Weaver, M. J. *Phys. Rev. B* 1991, 44, 10983.
- (22) Kolb, D. M.; Schneider, J. *Electrochim. Acta* 1986, 31, 929.
- (23) Honbo, H.; Itaya, K. *J. Chim. Phys.* 1991, 88, 1477.
- (24) Trevor, D. J.; Chidsey, C. E. D.; Loiacono, D. N. *Phys. Rev. Lett.* 1989, 62, 929.
- (25) Gewirth, A. A.; Bard, A. J. *J. Phys. Chem.* 1988, 92, 5563.
- (26) Kolb, D. M. In *Advances in Electrochemistry and Electrochemical Engineering*, Vol. 11; Gerischer, H., Tobias, C. W., Eds.; John Wiley & Sons: New York, 1984; p 125.
- (27) Magnussen, O. M.; Hotlos, J.; Nichols, R. J.; Kolb, D. M.; Behm, R. J. *Phys. Rev. Lett.* 1990, 64, 2929.
- (28) Magnussen, O. M.; Hotlos, J.; Beitel, G.; Kolb, D. M.; Behm, R. J. *J. Vac. Sci. Technol. B* 1991, 9, 969.
- (29) Hachiya, T.; Honbo, H.; Itaya, K. *J. Electroanal. Chem.* 1991, 315, 275.
- (30) Manne, S.; Hansma, P. K.; Massie, J.; Elings, V. B.; Gewirth, A. A. *Science* 1991, 251, 183.
- (31) Chen, C. H.; Vesey, S. M.; Gewirth, A. A. *J. Am. Chem. Soc.* 1992, 114, 451.
- (32) Chen, C. H.; Gewirth, A. A. *J. Am. Chem. Soc.* 1992, 114, 5439.
- (33) Chen, C. H.; Gewirth, A. A. *Phys. Rev. Lett.* 1992, 68, 1571.
- (34) Sashikata, K.; Furuya, N.; Itaya, K. *J. Electroanal. Chem.* 1991, 316, 361.
- (35) Hachiya, T.; Itaya, K. *Ultramicroscopy* 1992, 42–44, 445.
- (36) Yau, S. L.; Vitus, C. M.; Schardt, B. C. *J. Am. Chem. Soc.* 1990, 112, 3677.
- (37) Tao, N. J.; Lindsay, S. M. *J. Phys. Chem.* 1992, 96, 5213.
- (38) McCarley, R. L.; Bard, A. J. *J. Phys. Chem.* 1991, 95, 9618.
- (39) Gao, X.; Zhang, Y.; Weaver, M. J. *J. Phys. Chem.* 1992, 96, 4156.
- (40) Yau, S. L.; Gao, X.; Chang, S. C.; Schardt, B. C.; Weaver, M. J. *Am. Chem. Soc.* 1991, 113, 6049.
- (41) Vitus, C. M.; Chang, S. C.; Schardt, B. C.; Weaver, M. J. *J. Phys. Chem.* 1991, 95, 7559.
- (42) Schott, J. H.; Arana, C. R.; Abrufa, H. D.; Petoch, H. H.; Elliot, G. M.; White, H. S. *J. Phys. Chem.* 1992, 96, 5222.
- (43) Widrig, C. A.; Alves, C. A.; Porter, M. C. *J. Am. Chem. Soc.* 1991, 113, 2805.
- (44) Haussling, L.; Michel, B.; Ringsdorf, H.; Rohrer, H. *Angew. Chem., Int. Ed. Engl.* 1991, 30, 569.
- (45) Kim, Y.-T.; McCarley, R. L.; Bard, A. J. *J. Phys. Chem.* 1992, 96, 7416.
- (46) Hubbard, A. T. *Langmuir* 1990, 6, 97.
- (47) Higashi, G. S.; Becker, R. S.; Chabel, Y. J.; Becker, A. J. *Appl. Phys. Lett.* 1991, 58, 1656.
- (48) Itaya, K.; Sugawara, R.; Morita, Y.; Talumoto, H. *Appl. Phys. Lett.* 1992, 60, 2534.
- (49) Yau, S.-L.; Fan, F.-R. F.; Bard, A. J. *J. Electrochem. Soc.* 1992, 139, 2825.
- (50) Tomita, E.; Matsuda, N.; Itaya, K. *J. Vac. Sci. Technol. A* 1990, 8, 534.
- (51) Fan, F.-R. F.; Bard, A. J. *J. Phys. Chem.* 1990, 94, 3761.
- (52) Fan, F.-R.; Bard, A. J. *J. Phys. Chem.* 1991, 95, 1969.
- (53) Dubois, D.; Kadish, K. M.; Flanagan, S.; Haufler, R. E.; Chibante, L. P. F.; Wilson, L. J. *J. Am. Chem. Soc.* 1991, 113, 4364.
- (54) Flarsheim, W. M.; Bard, A. J.; Johnston, K. P. *J. Phys. Chem.* 1989, 93, 4234.
- (55) *Microelectrodes: Theory and Applications*; Montenegro, M. I.; Querós, M. A.; Daschback, J. L., Eds.; NATO ASI Series E, Vol. 197; Kluwer: Dordrecht, 1991.
- (56) Wightman, R. M.; Wipf, D. O. In *Electroanalytical Chemistry*, Vol. 15; A. J. Bard, Ed.; Marcel Dekker: New York, 1989; p 267.
- (57) Morris, R. B.; Franta, D. J.; White, H. S. *J. Phys. Chem.* 1987, 91, 3559.
- (58) Bard, A. J.; Denuault, G.; Lee, C.; Mandler, D.; Wipf, D. O. *Acc. Chem. Res.* 1990, 23, 357.
- (59) Bard, A. J.; Fan, F.-R. F.; Pierce, D. T.; Unwin, P. R.; Wipf, D. O.; Zhou, F. *Science* 1991, 254, 68.
- (60) Mirkin, M.; Fan, F.-R. F.; Bard, A. J. *Science* 1992, 257, 364.
- (61) Scott, E. R.; White, H. S.; Phipps, B. J. *Membrane Sci.* 1991, 58, 71.
- (62) Scott, E. R.; White, H. S.; Phipps, B. *Solid State Ionics* 1992, 53–56, 176.
- (63) *Electrochemical Interfaces: Modern Techniques for In-Situ Interface Characterization*; Abrufa, H. D., Ed.; VCH Verlag Chemical: New York, 1991.
- (64) Abrufa, H. D. *Adv. Chem. Phys.* 1990, 77, 255.
- (65) Lee, P. A.; Citrin, P. H.; Eisenberger, P.; Kincaid, B. M. *Rev. Mod. Phys.* 1981, 53, 769.
- (66) *EXAFS Spectroscopy: Techniques and Applications*; Teo, B. K., Joy, D. C., Eds.; Plenum: New York, 1981.
- (67) Teo, B. K. *EXAFS: Basic Principles and Data Analysis*; Springer Verlag: Berlin, 1986.
- (68) Abrufa, H. D.; White, J. H.; Albarelli, M. J.; Bommarito, G. M.; Bedzyk, M. J.; McMillan, M. *J. Phys. Chem.* 1988, 92, 7045.
- (69) Melroy, O. R.; Samant, M. G.; Borges, G. L.; Gordon, J. G.; Blum, L.; White, J. H.; Albarelli, M. J.; McMillan, M.; Abrufa, H. D. *Langmuir* 1988, 4, 728.
- (70) Tourillon, G.; Guay, D.; Tadjeddine, A. *J. Electroanal. Chem.* 1990, 289, 263.
- (71) Tadjeddine, A. J.; Guay, D.; Ladouceur, M.; Tourillon, G. *Phys. Rev. Lett.* 1991, 66, 2235.
- (72) Samant, M. G.; Borges, G. L.; Gordon, J. G.; Melroy, O. R.; Blum, L. *J. Am. Chem. Soc.* 1987, 109, 5970.
- (73) McBreen, J.; O'Grady, W. E.; Pandya, K. I.; Hoffman, R. W.; Sayers, D. E. *Langmuir* 1986, 3, 428.
- (74) Dartige, E.; Fonatine, A.; Tourillon, G.; Jucha, A. *Jnl. de Phys. Colloque* 1986, 47, 607.
- (75) Martens, G.; Rabe, P. *Phys. Stat. Solidi A* 1980, 58, 415.
- (76) Toney, M.; Gordon, J.; Samant, M.; Borges, G.; Wiesler, D.; Yee, D.; Sorensen, L. *Langmuir* 1991, 7, 796.
- (77) Toney, M.; Gordon, J.; Kau, L.; Borger, G.; Melroy, O.; Samant, M.; Wiesler, D.; Yee, D.; Sorensen, L. *Phys. Rev. B* 1990, 42, 5594.
- (78) Melroy, O.; Toney, M.; Borges, G.; Samant, M.; Kortright, J.; Ross, P.; Blum, L. *J. Electroanal. Chem.* 1989, 258, 403.
- (79) Melroy, O.; Toney, M.; Borges, G.; Samant, M.; Kortright, J.; Ross, P.; Blum, L. *Phys. Rev. B* 1988, 38, 10962.
- (80) Samant, M.; Toney, M.; Borges, G.; Blum, L.; Melroy, O. *J. Phys. Chem.* 1988, 92, 200.
- (81) Samant, M.; Toney, M.; Borges, G.; Blum, L.; Melroy, O. *Surf. Sci.* 1988, 193, 129.
- (82) Toney, M.; Gordon, J.; Samant, M.; Borges, G.; Melroy, O. *Phys. Rev. B* 1992, 45, 9362.
- (83) Ocko, B.; Wang, J.; Davenport, A.; Isaacs, H. *Phys. Rev. Lett.* 1992, 68, 1466.
- (84) Wang, J.; Davenport, A.; Isaacs, H.; Ocko, B. *Science* 1992, 255, 1416.
- (85) Ocko, B.; Gibaud, A.; Wang, J. *J. Vac. Sci. Technol. A* 1992, 10, 3019.
- (86) Wang, J.; Ocko, B.; Davenport, A.; Isaacs, H. *Phys. Rev. B* 1992, 46, 10321.
- (87) Hamelin, A. *J. Electroanal. Chem.* 1982, 142, 299.
- (88) Robinson, J. *Phys. Rev. B* 1986, 33, 3830.
- (89) Batterman, B. W.; Cole, H. *Rev. Mod. Phys.* 1964, 36, 681.
- (90) Materlik, G.; Zegenhagen, J.; Uelhoff, W. *Phys. Rev. B* 1985, 32, 5502.
- (91) Materlik, G.; Schmah, M.; Zegenhagen, J.; Uelhoff, W. *Bunsen-Ges. Phys. Chem.* 1987, 91, 292.
- (92) Bedzyk, M. J.; Bilderback, D.; White, J. H.; Abrufa, H. D.; Bommarito, G. M. *J. Phys. Chem.* 1986, 90, 4926.
- (93) Bommarito, G. M.; White, J. H.; Abrufa, H. D. *J. Phys. Chem.* 1990, 94, 8280.
- (94) Bommarito, G. M.; Acevedo, D.; Rodriguez, J. F.; Abrufa, H. D. In *X-Rays in Materials Analysis: Novel Applications and Recent Developments, SPIE Proceedings*, Vol. 1550; Mills, D. M., Ed.; The International Society for Optical Engineering: Bellingham, WA, 1991; p 156.
- (95) Shen, Y. *The Principles of Nonlinear Optics*; John Wiley & Sons: New York, 1984.
- (96) Richmond, G. In *Advances in Electrochemical Science and Engineering*, Vol. 2; Gerischer, H., Tobias, C., Eds.; VCH Verlag Chemical: New York, 1990; p 142.
- (97) Richmond, G. In *Electrochemical Interfaces, Modern Techniques for In-Situ Interface Characterization*; Abrufa, H., Ed.; VCH: Berlin, 1991; p 265.
- (98) Richmond, G. L. In *Electroanalytical Chemistry*; A. J. Bard, Ed.; Marcel Dekker: New York, 1991; p 87.
- (99) Koos, D.; Richmond, G. *J. Phys. Chem.* 1992, 96, 3770.

- (100) Georgiadis, R.; Richmond, G. *J. Phys. Chem.* **1991**, *95*, 2895.
 (101) Hubbard, A. T. *Accs. Chem. Res.* **1980**, *13*, 177.
 (102) Ross, P. N. In *Chemistry and Physics of Solid Surfaces, Vol IV*; Vanselow, R., Howe, R., Eds.; Springer-Verlag: New York, 1982; p 173.
 (103) Yeager, E.; Homa, A.; Cahan, B. D.; Scherson, D. *J. Vac. Sci. Technol.* **1982**, *20*, 628.
 (104) Kolb, D. M. *Z. Phys. Chem. Neue Folge.* **1987**, *154*, 179.
 (105) Sass, J. K.; Bange, K. In *Electrochemical Surface Science*; Soriaga, M. P., Ed.; American Chemical Society: Washington, DC., 1988; p 54.
 (106) Wagner, F. T.; Moylan, T. E. In *Electrochemical Surface Science*; Soriaga, M. P., Ed.; American Chemical Society: Washington, D.C., 1988; p 65.
 (107) Hansen, W. N. *J. Electroanal. Chem.* **1983**, *150*, 133.
 (108) Hansen, W. N.; Hansen, G. J. In *Electrochemical Surface Science*; Soriaga, M. P., Ed.; American Chemical Society: Washington, D.C., 1988; p 166.
 (109) Pemberton, J. E.; Sobocinski, R. L.; Bryant, M. A. *J. Am. Chem. Soc.* **1990**, *112*, 6177.
 (110) Ross, P. N. *J. Chim. Phys.* **1991**, *88*, 1353.
 (111) Faguy, P.; Markovic, N.; Adzic, R.; Fieiro, C.; Yeager, E. *J. Electroanal. Chem.* **1990**, *289*, 245.
 (112) Bravo, B. G.; Michelhaugh, S. L.; Soriaga, M. P.; Villegas, I.; Suggs, D. W.; Stickney, J. L. *J. Phys. Chem.* **1991**, *95*, 5245.
 (113) Gao, X.; Weaver, M. J. *J. Am. Chem. Soc.* **1992**, *114*, 8544.
 (114) Stickney, J. L.; Rosasco, S. D.; Soriaga, M. P.; Song, D.; Hubbard, A. T. *Surf. Sci.* **1983**, *130*, 326.
 (115) Andricacos, P. C.; Ross, P. N. *J. Electroanal. Chem.* **1984**, *167*, 301.
 (116) Aberdam, D.; Durand, R.; Faure, R.; El-Omar, F. *Surf. Sci.* **1985**, *162*, 782.
 (117) Leung, L. W. H.; Gregg, T. W.; Goodman, D. W. *Langmuir* **1991**, *7*, 3205.
 (118) Laguren-Davidson, L.; Lu, F.; Salaita, G. N.; Hubbard, A. T. *Langmuir* **1988**, *4*, 224.
 (119) Hanson, M. E.; Yeager, E. In *Electrochemical Surface Science*; Soriaga, M. P., Ed.; American Chemical Society: Washington, D.C., 1988; p 141.
 (120) Goodman, D. W.; Stuve, E. M. In *Electrochemical Surface Science*; Soriaga, M. P., Ed.; American Chemical Society: Washington, D.C., 1988; p 154.
 (121) Suggs, D. W.; Villegas, I.; Gregory, B. W.; Stickney, J. L. *Mater. Res. Soc. Symp. Proc.* **1991**, *222*, 283.
 (122) Thiel, P. A.; Maday, T. E. *Surf. Sci. Rep.* **1987**, *7*, 211.
 (123) Zurawski, D.; Wasberg, M.; Wieckowski, A. *J. Phys. Chem.* **1990**, *94*, 2076.
 (124) Berry, G. M.; Bothwell, M. E.; Michelhaugh, S. L.; McBride, J. R.; Soriaga, M. P. *J. Chim. Phys.* **1991**, *88*, 1591.
 (125) Salaita, G. N.; Hubbard, A. T. In *Techniques of Chemistry: Molecular Design of Electrode Surfaces*; Murray, R. W., Ed.; John Wiley & Sons: New York, 1989; p 49.
 (126) Gui, J. Y.; Lu, F.; Stern, D. A.; Hubbard, A. T. *J. Electroanal. Chem.* **1990**, *292*, 245.
 (127) Tabor, D.; Winterton, R. H. S. *Nature* **1968**, *219*, 1120.
 (128) Israelachvili, J. N.; McGuigan, P. M.; Homola, A. M.; Homola, A. M. *Science* **1988**, *240*, 248.
 (129) Smith, C. P.; Snyder, S. R.; White, H. S. In *Electrochemical Interfaces*; Abruna, H. D., Ed.; VCH Verlag Chemical: New York, 1991; p 157.
 (130) Claesson, P.; Horn, R. G.; Pashley, R. M. *J. Coll. Int. Sci.* **1984**, *100*, 250.
 (131) Israelachvili, J. N. *Chem. Scrip.* **1985**, *25*, 1.
 (132) Parker, J. L.; Christenson, H. K. *J. Chem. Phys.* **1988**, *88*, 8013.
 (133) Pashley, R. M. *Chem. Scrip.* **1985**, *25*, 7.
 (134) Chen, T. T.; Chang, R. K. *Surf. Sci.* **1985**, *158*, 325.
 (135) Tang, Z.; Mier-y-Tang, L.; Davis, H. T.; Scriven, L. E.; White, H. S. *Mol. Phys.* **1991**, *71*, 369.
 (136) Schmickler, W.; Henderson, D. *Prog. Surf. Sci.* **1986**, *22*, 323.
 (137) Carnie, S. L. *Ber. Bunsen-Ges. Phys. Chem.* **1987**, *91*, 262.
 (138) Torrie, G. M.; Valleau, J. P. *J. Phys. Chem.* **1982**, *86*, 3251.
 (139) Torrie, G. M.; Kusalik, P. G.; Patey, G. N. *J. Chem. Phys.* **1988**, *89*, 3285.
 (140) Heinzinger, K.; Spohr, E. *Electrochim. Acta* **1989**, *34*, 1849.
 (141) Lee, C. Y.; McCommon, J. A.; Rossky, P. J. *J. Chem. Phys.* **1984**, *80*, 4448.
 (142) Glosli, J. N.; Philpott, M. J. *Chem. Phys.* **1992**, *96*, 6962.
 (143) Curtiss, L. A.; Halley, J. W.; Hautman, J.; Hung, N. C.; Nagy, Z.; Rhee, Y. J.; Yonco, R. M. *J. Electrochem. Soc.* **1991**, *138*, 2032.
 (144) Bard, A. J.; Faulkner, L. R. *Electrochemical Methods: Fundamentals and Applications*; John Wiley & Sons: New York, 1980; pp 100–107.
 (145) Safford, L. K.; Weaver, M. J. *J. Electroanal. Chem.* **1992**, *331*, 857.
 (146) Deakin, M. R.; Wightman, R. M.; Amatore, C. A. *J. Electroanal. Chem.* **1986**, *215*, 49.
 (147) Oldham, K. B.; Zoski, C. G. *J. Electroanal. Chem.* **1988**, *256*, 11.
 (148) Michael, A. C.; Wightman, R. M.; Amatore, C. A. *J. Electroanal. Chem.* **1987**, *267*, 33.
 (149) Amatore, C. A.; Deakin, M. R.; Wrightman, R. M. *J. Electroanal. Chem.* **1986**, *206*, 23.
 (150) Delahay, P. *New Instrumental Methods in Electrochemistry*; John Wiley & Sons: New York, 1954; pp 67–70.
 (151) Garreau, D.; Hapiot, P.; Saveant, J.-M. *J. Electroanal. Chem.* **1990**, *281*, 73.
 (152) Amatore, C.; Lefrou, C.; Pfluger, F. *J. Electroanal. Chem.* **1989**, *270*, 43.
 (153) Andrieux, C. P.; Hapiot, P.; Saveant, J.-M. *J. Phys. Chem.* **1988**, *92*, 5992.
 (154) Faulkner, L. R.; Walsh, M. R.; Xu, C. In *Contemp. Electroanal. Chem.*; Ivaska, A.; Lewenstam, A.; Sara, R., Eds.; Plenum: New York, 1990; p 5.
 (155) Andrieux, C. P.; Garreau, D.; Hapiot, P.; Pinson, J.; Saveant, J.-M. *J. Electroanal. Chem.* **1988**, *243*, 321.
 (156) Andrieux, C. P.; Hapiot, P.; Saveant, J.-M. *Chem. Rev.* **1990**, *90*, 723.
 (157) Bard, A. J.; Faulkner, L. R. *Electrochemical Methods: Fundamentals and Applications*; John Wiley & Sons: New York, 1980; pp 222–224, 523–525.
 (158) Becka, A. M.; Miller, C. J. *J. Phys. Chem.* **1992**, *96*, 2657.
 (159) Schmickler, W. J. *Electroanal. Chem.* **1986**, *204*, 31.
 (160) Zusman, L. D. *Chem. Phys.* **1987**, *112*, 53.
 (161) Chidsey, C. E. D. *Science* **1991**, *251*, 919.
 (162) Rudolph, M. J. *Electroanal. Chem.* **1991**, *314*, 13.
 (163) Britz, D. *Digital Simulation in Electrochemistry: Second, Revised and Extended Edition*; Springer-Verlag: Berlin, 1988.
 (164) Wipf, D. O.; Kristensen, E. W.; Deakin, M. R.; Wightman, R. M. *J. Electroanal. Chem.* **1988**, *60*, 306.
 (165) Pendley, B. D.; Abruna, H. D. *Anal. Chem.* **1990**, *62*, 782.
 (166) Penner, R. M.; Heben, M. J.; Longin, T. L.; Lewis, N. S. *Science* **1990**, *250*, 1118.
 (167) Oldham, K. B.; Myland, J. C.; Zoski, C. G.; Bond, A. M. *J. Electroanal. Chem.* **1989**, *270*, 79.
 (168) Mirkin, M. V.; Bard, A. J. *J. Anal. Chem.* **1992**, *64*, 2293.
 (169) Amatore, C.; Lefrou, C. *J. Electroanal. Chem.* **1990**, *296*, 335.
 (170) Norton, J. D.; White, H. S.; Feldberg, S. W. *J. Phys. Chem.* **1990**, *94*, 6772.
 (171) Cooper, J. B.; Bond, A. M.; Oldham, K. B. *J. Electroanal. Chem.* **1992**, *331*, 877.
 (172) Seibold, J. D.; Scott, E. R.; White, H. S. *J. Electroanal. Chem.* **1989**, *264*, 281.
 (173) Sabatani, E.; Rubinstein, I. *J. Phys. Chem.* **1987**, *91*, 6663.
 (174) Bailiwicks, R.; Majda, M. *J. Am. Chem. Soc.* **1991**, *113*, 5464.
 (175) Reller, H.; Kirowa-Eisner, E.; Gileadi, E. *J. Electroanal. Chem.* **1982**, *58*, 5321.
 (176) Amatore, C.; Saveant, J.-M.; Tessier, D. *J. Electroanal. Chem.* **1983**, *147*, 39.
 (177) Wipf, D. O.; Bard, A. J. *J. Electrochem. Soc.* **1991**, *138*, 469.
 (178) Mirkin, M. V.; Bard, A. J. *J. Electroanal. Chem.* **1992**, *323*, 1.
 (179) Mirkin, M. V.; Richards, T.; Bard, A. J. *J. Phys. Chem.*, in press.
 (180) Axup, A. W.; Albin, M.; Mayo, S. L.; Crutchley, R. J.; Gray, H. B. *J. Am. Chem. Soc.* **1988**, *110*, 435.
 (181) Miller, C.; Cuendet, P.; Gratzel, M. *J. Phys. Chem.* **1991**, *95*, 877.
 (182) Miller, C.; Gratzel, M. *J. Phys. Chem.* **1991**, *95*, 5225.
 (183) Saveant, J.-M. *J. Electroanal. Chem.* **1991**, *302*, 91.
 (184) Feldberg, S. W.; Smalley, J. F.; Chidsey, C. E. D. *Book of Abstracts*, Pittsburgh Conference on Analytical Chemistry and Applied Spectroscopy, New Orleans, LA; The Society for Analytical Chemists of Pittsburgh and the Spectroscopy Society of Pittsburgh; Pittsburgh, PA, 1992, No. 825.
 (185) Finklea, H.; Hanshew, D. D. *J. Am. Chem. Soc.* **1992**, *114*, 3173.
 (186) Benderski, V. A.; Babenko, S. D.; Krivenko, A. G. *J. Electroanal. Chem.* **1978**, *86*, 223.
 (187) Benderski, V. A.; Velichko, G. I. *J. Electroanal. Chem.* **1982**, *140*, 1.
 (188) Smalley, J. F.; Krisnan, C. V.; Goldman, M.; Feldberg, S. W.; Ruzic, I. *J. Electroanal. Chem.* **1988**, *248*, 255.
 (189) van Leeuwen, H. P. In *Electroanalytical Chemistry, Vol. 12*; Bard, A. J., Ed.; Marcel Dekker: New York, 1966; p 159.
 (190) Coufal, H. *Appl. Phys. Lett.* **1983**, *44*, 59.
 (191) Coufal, H.; Hefferle, P. *Appl. Phys. A* **1985**, *38*, 213.
 (192) Bewick, A.; Pons, S. In *Advances in Infrared and Raman Spectroscopy, Vol. 4*; Clarke, R., Hester, R., Eds.; Heyden: Philadelphia, 1985; Ch 1.
 (193) Bryant, M. A.; Job, S. L.; Pemberton, J. E. *Langmuir* **1992**, *8*, 753.
 (194) Gottesfeld, S. In *Electroanalytical Chemistry, Vol. 15*; Bard, A. J., Ed.; Marcel Dekker: New York, 1989; p 143.
 (195) Gomez-Jahn, L. A.; Miller, R. J. D. *J. Chem. Phys.* **1992**, *96*, 3981.
 (196) Miller, R. J. D. *Report, DOE/ER/13455-4*; U.S. Department of Energy, Energy Res. Abstr. 1991, *16*(7), Abstr. No. 17678 (Eng) 1990, Order No. DE91010914.
 (197) Finklea, H. O.; Hanshew, D. D. *J. Am. Chem. Soc.* **1992**, *114*, 3173.
 (198) Kuki, A. In *Structure and Bonding, Vol 75: Long-Range Electron Transfer in Biology*; Clarke, M. J., Goodenough, J. B., Jorgensen, C. K., Neilands, J. B., Reinen, D., Weiss, R., Eds.; Springer-Verlag: New York, 1991; p 49.
 (199) Jordan, K. D.; Paddison-Row, M. N. *J. Phys. Chem.* **1992**, *96*, 1188.
 (200) Liang, C.; Newton, M. D. *J. Phys. Chem.* **1992**, *96*, 2855.
 (201) Naleway, C. A.; Curtiss, L. A.; Miller, J. R. *J. Phys. Chem.* **1991**, *95*, 8434.
 (202) Siddarth, P.; Marcus, R. A. *J. Phys. Chem.* **1992**, *96*, 3213.
 (203) Ratner, M. A. *J. Phys. Chem.* **1990**, *94*, 4877.

- (204) Beratan, D. N.; Betts, J. N.; Onuchic, J. N. *J. Phys. Chem.* **1992**, *96*, 2852.
- (205) Bard, A. J.; Faulkner, L. R. *Electrochemical Methods: Fundamentals and Applications*; John Wiley & Sons: New York, 1980; pp 542-543.
- (206) Smith, C. P.; White, H. S. *Anal. Chem.* **1992**, *64*, 2398.
- (207) Chidsey, C. E. D.; Murray, R. W. *Science* **1986**, *231*, 25.
- (208) Creager, S. E.; Collard, D. M.; Fox, M. A. *Langmuir* **1990**, *6*, 1617.
- (209) Heller, A. *Acc. Chem. Res.* **1990**, *23*, 128.
- (210) Heller, A. *J. Phys. Chem.* **1992**, *96*, 3579.
- (211) Oppenheim, I. C.; Trevor, D. J.; Chidsey, C. E. D.; Trevor, P. L.; Sieradzki, K. *Science* **1991**, *254*, 687.
- (212) McCarley, R. L.; Bard, A. J. *J. Phys. Chem.* **1992**, *96*, 7410.
- (213) *Molecular Design of Electrode Surfaces, Techniques of Chemistry Series, Vol. 22*; Murray, R. W., Ed.; John Wiley & Sons: New York, 1992.
- (214) Parsons, R.; VanderNoot, T. J. *Electroanal. Chem.* **1988**, *257*, 9.
- (215) Tang, S. L.; Kasowski, R. V.; Parkinson, B. A. *Phys. Rev. B* **1989**, *39*, 9987.
- (216) Coleman, R. V.; Drake, B.; Hansma, P. K.; Slough, G. *Phys. Rev. Lett.* **1985**, *55*, 394.
- (217) Wu, L.-L.; Zhou, P.; Lieber, C. M. *Nature* **1988**, *35*, 55.
- (218) (a) Olson, J.; Kurtz, S.; Kibbler, A.; Faine, P. *Appl. Phys. Lett.* **1990**, *56*, 623. (b) Chung, C.; Virshup, G.; Hikido, S.; Kaminar, N. *Appl. Phys. Lett.* **1989**, *55*, 1741.
- (219) Pinkowski, A.; Jüttner, K.; Lorenz, W. J. *J. Electroanal. Chem.* **1990**, *287*, 203.
- (220) Pinkowski, A.; Jüttner, K.; Lorenz, W. J.; Saemann-Ischenko, G.; Breiter, M. W. *J. Electroanal. Chem.* **1990**, *286*, 253.
- (221) Pinkowski, A.; Doneit, J.; Jüttner, K.; Lorenz, W. J.; Saemann-Ischenko, G.; Zetterer, T.; Breiter, M. W. *Electrochim. Acta* **1989**, *34*, 1113.
- (222) Breiter, M. W.; Lorenz, W. J.; Saemann-Ischenko, G. *Surf. Sci.* **1990**, *230*, 213.
- (223) Lorenz, W. J.; Saemann-Ischenko, G.; Breiter, M. W. *Bunsen-Ges. Phys. Chem.* **1991**, *95*, 1055.
- (224) Peck, S. R.; Curtin, L. S.; McDevitt, J. T.; Murray, R. W.; Collman, J. P.; Little, W. A.; Zetterer, T.; Duan, H. M.; Dong, C.; Hermann, A. M. *J. Am. Chem. Soc.* **1992**, *114*, 6771.
- (225) Kuznetsov, A. M. *J. Electroanal. Chem.* **1990**, *278*, 1.
- (226) Zusman, L. D.; Gelman, A. B.; Shapiro, B. *Chem. Phys. Lett.* **1990**, *167*, 457.
- (227) Jaeger, C. D.; Bard, A. J. *J. Am. Chem. Soc.* **1979**, *101*, 1690.
- (228) Ward, M. D. In *Electroanalytical Chemistry, Vol. 16*; Bard, A. J., Ed.; Marcel Dekker: New York, 1989, p 220.
- (229) Ward, M. D. *Electroanal. Chem.* **1989**, *16*, 181.
- (230) Ward, M. D.; Fagan, P. J.; Calabrese, J. C.; Johnson, D. C. *J. Am. Chem. Soc.* **1989**, *111*, 1719.
- (231) Rosamilia, J.; Miller, B. J. *Electrochim. Soc.* **1989**, *136*, 1053.
- (232) *Physics of X-Ray Multilayer Structures*; Kortright, J.; Sterns, D.; Windt, D., Eds.; The Optical Society of America: Washington, D.C., 1992.
- (233) Porat, O.; Riess, I.; Tuller, H. *Physica C* **1992**, *192*, 60.
- (234) Ross, P. In *Structure of Electrified Interfaces*; Lipkowski, J.; Ross, P., Eds.; VCH: New York, 1993; p 35.
- (235) Murray, R. W. In *Electroanalytical Chemistry, Vol. 13*; Bard, A. J., Ed.; Marcel Dekker: New York, 1984; p 191.
- (236) Murray, R. W. *Acc. Chem. Res.* **1980**, *13*, 135.
- (237) Murray, R. W. *Ann. Rev. Mater. Sci.* **1984**, *14*, 145.
- (238) Abrufa, H. D. In *Electroresponsive Molecular and Polymeric Systems*; Skotheim, T., Ed.; Marcel Dekker: New York, 1988; p 97.
- (239) Facci, J. S. In *Techniques of Chemistry Series, Vol. 22*; John Wiley & Sons: New York, 1992; p 119.
- (240) Ulman, A. *An Introduction to Ultrathin Organic Films From Langmuir-Blodgett To Self-Assembly*; Academic Press: San Diego, 1991.
- (241) Stern, D. A.; Lagun-Davidson, L.; Frank, D. G.; Gui, J. Y.; Lin, C.-H.; Lu, F.; Salaita, G. N.; Walton, N.; Zapien, D. C.; Hubbard, A. T. J. *Am. Chem. Soc.* **1989**, *111*, 877.
- (242) Bain, C. D.; Whitesides, G. M. *Angew. Chem.* **1989**, *101*, 506.
- (243) Dubois, L.; Nuzzo, R. G. *Ann. Rev. Phys. Chem.* **1992**, *43*, 437.
- (244) Nuzzo, R. G.; Fusco, F.; Allara, D. L. *J. Am. Chem. Soc.* **1987**, *109*, 2358.
- (245) Porter, M. D.; Bright, T. B.; Allara, D. L.; Chidsey, C. E. D. *J. Am. Chem. Soc.* **1987**, *109*, 3559.
- (246) Bain, C. D.; Troughton, E. B.; Tao, Y.-T.; Evall, J.; Whitesides, G. M.; Nuzzo, R. G. *J. Am. Chem. Soc.* **1989**, *111*, 321.
- (247) Troughton, E. B.; Bain, C. D.; Whitesides, G. M.; Nuzzo, R. G.; Allara, D. L.; Porter, M. D. *Langmuir* **1988**, *4*, 365.
- (248) Mebrahtu, T.; Berry, G. M.; Bravo, B. G.; Michelhaugh, S. L.; Soriaga, M. P. *Langmuir* **1988**, *4*, 1147.
- (249) Hickman, J. J.; Ofer, D.; Zou, C.; Wrighton, M. S.; Laibinis, P. E.; Whitesides, G. M. *J. Am. Chem. Soc.* **1991**, *113*, 1128.
- (250) Creager, S. E.; Hockett, L. A.; Rowe, G. K. *Langmuir* **1992**, *8*, 854.
- (251) Nuzzo, R. G.; Dubois, L. H.; Allara, D. A. *J. Am. Chem. Soc.* **1990**, *112*, 558.
- (252) Chidsey, C. E. D.; Loiacano, D. N. *Langmuir* **1990**, *6*, 682.
- (253) Popeno, D. D.; Deinhammer, R. S.; Porter, M. D. *Langmuir* **1992**, *8*, 2521.
- (254) Bain, C. D.; Biebuyck, H. A.; Whitesides, G. M. *Langmuir* **1989**, *5*, 723.
- (255) Bryant, M. A.; Pemberton, J. E. *J. Am. Chem. Soc.* **1991**, *113*, 8284.
- (256) Carron, K. T.; Hurley, L. G. *J. Phys. Chem.* **1991**, *95*, 9979.
- (257) Chidsey, C. E. D.; Liu, G.-Y.; Rountree, P.; Scoles, G. *J. Chem. Phys.* **1989**, *91*, 4421.
- (258) Strong, L.; Whitesides, G. M. *Langmuir* **1988**, *4*, 546.
- (259) Alves, C. A.; Smith, E. L.; Porter, M. D. *J. Am. Chem. Soc.* **1992**, *114*, 1222.
- (260) Alves, C. A.; Smith, E. L.; Porter, M. D. *J. Am. Chem. Soc.* **1992**, *114*, 1222.
- (261) Chidsey, C. E. D.; Bertozi, C. R.; Putvinski, T. M.; Muisce, A. M. *J. Am. Chem. Soc.* **1990**, *112*, 4301.
- (262) Bain, C. D.; Whitesides, G. M. *J. Am. Chem. Soc.* **1989**, *111*, 7164.
- (263) Wang, J.; Frostman, L. M.; Ward, M. D. *J. Phys. Chem.* **1992**, *96*, 5224.
- (264) Li, Y.; Huang, J.; McIver, R. T., Jr.; Hemminger, J. C. *J. Am. Chem. Soc.* **1992**, *114*, 2428.
- (265) Finklea, H. O.; Avery, S.; Lynch, M. *Langmuir* **1987**, *3*, 409.
- (266) Collard, D. M.; Fox, M. A. *Langmuir* **1991**, *7*, 1192.
- (267) Sun, L.; Crooks, R. M. *J. Electrochem. Soc.* **1991**, *138*, L23.
- (268) Stole, S. M.; Widrig, C. A.; Porter, M. D. In *Third International Symposium on Chemically Modified Surfaces*; Leyden, D.; Collins, W., Eds.; Gordon and Breach: New York, 1990; p 333.
- (269) Steinberg, S.; Tor, Y.; Sabatani, E.; Rubinstein, I. *J. Am. Chem. Soc.* **1991**, *113*, 5176.
- (270) Finklea, H. O.; Snider, D. A.; Fedyk, J. *Langmuir* **1990**, *6*, 371.
- (271) Rubinstein, I.; Steinberg, S.; Tor, Y.; Shanzer, A.; Sagiv, J. *Nature* **1988**, *332*, 426.
- (272) Rowe, G. K.; Creager, S. E. *Langmuir* **1991**, *7*, 2307.
- (273) Nordyke, L. L.; Buttry, D. A. *Langmuir* **1991**, *7*, 380.
- (274) Tarlov, M. J.; Bowden, E. F. *J. Am. Chem. Soc.* **1991**, *113*, 1847.
- (275) Acevedo, D.; Abrufa, H. D. *J. Phys. Chem.* **1991**, *95*, 9590.
- (276) Netzer, L.; Sagiv, J. *J. Am. Chem. Soc.* **1983**, *105*, 674.
- (277) Tillman, N.; Ulman, A.; Penner, T. *Langmuir* **1989**, *5*, 101.
- (278) Lee, H.; Kepley, L. J.; Hong, H.-G.; Akhter, S.; Mallouk, T. E. *J. Phys. Chem.* **1988**, *92*, 2597.
- (279) Li, D.; Ratner, M. A.; Marks, T. J.; Zhang, C.; Yang, J.; Wong, G. K. *J. Am. Chem. Soc.* **1990**, *112*, 7389.
- (280) Hong, H.-G.; Mallouk, T. E. *Langmuir* **1991**, *7*, 2362.
- (281) Evans, S. D.; Ulman, A.; Goppert-Berarducci, K. E.; Gerenser, L. *J. Am. Chem. Soc.* **1991**, *113*, 5866.
- (282) Curtin, L. S.; Peck, S. R.; Tender, L. M.; Murray, R. W.; Rowe, G. K.; Creager, S. E. *Anal. Chem.* **1993**, *65*, 386.
- (283) Popeno, D. D.; Stole, S. M.; Porter, M. D. *Appl. Spectrosc.* **1992**, *46*, 79.
- (284) Bain, C. D.; Evall, J.; Whitesides, G. M. *J. Am. Chem. Soc.* **1989**, *111*, 7155.
- (285) Sheen, C. W.; Shi, J.-X.; Martensson, J.; Parikh, A. N.; Allara, D. L. *J. Am. Chem. Soc.* **1992**, *114*, 1514.
- (286) Kwan, W. S. V.; Atanasoska, L.; Miller, L. L. *Langmuir* **1991**, *7*, 1419.
- (287) Katz, E. Y.; Solov'ev, A. A. *J. Electroanal. Chem.* **1990**, *291*, 171.
- (288) Haussling, L.; Ringsdorf, H.; Schmitt, F.-J.; Knoll, W. *Langmuir* **1991**, *7*, 1837.
- (289) Tengvall, P.; Lestelius, M.; Liedberg, B.; Lundstrom, I. *Langmuir* **1992**, *8*, 1236.
- (290) Duevel, R. V.; Corn, R. M. *Anal. Chem.* **1992**, *64*, 337.
- (291) Dulcey, C. S.; Georger, J. H., Jr.; Krauthamer, V.; Stenger, D. A.; Fare, T. L.; Calvert, J. M. *Science* **1991**, *252*, 551.
- (292) Fujihira, M. In *Topics in Organic Electrochemistry*; Fry, A. J.; Britton, W. E., Eds.; Plenum: New York, 1986; p 255.
- (293) Merz, A. In *Topics in Current Chemistry, Vol. 152*; Springer Verlag: Berlin, 1990; p 49.
- (294) Hughes, R. C.; Ricco, A. J.; Butler, M. A.; Martin, S. J. *Science* **1991**, *254*, 74.
- (295) Watkins, B. F.; Behling, J. R.; Kariv, E.; Miller, L. L. *J. Am. Chem. Soc.* **1975**, *97*, 3549.
- (296) Komari, T.; Nonaka, T. *J. Am. Chem. Soc.* **1984**, *106*, 2656.
- (297) Matsue, T.; Fujihira, M.; Osa, T. *J. Electrochem. Soc.* **1981**, *128*, 1473.
- (298) Yamagishi, A.; Aramata, A. *J. Chem. Soc., Chem. Commun.* **1984**, *7*, 452.
- (299) Nakashima, N.; Tajuchi, T.; Takada, Y.; Fujio, K.; Kunitake, M.; Manabe, O. *J. Chem. Soc., Chem. Commun.* **1991**, *4*, 232.
- (300) Sun, L.; Johnson, B.; Wade, T.; Crooks, R. M. *J. Phys. Chem.* **1990**, *94*, 8869.
- (301) Nagase, S.; Kataoka, M.; Naganawa, R.; Komatsu, R.; Odashima, K.; Umezawa, Y. *Anal. Chem.* **1990**, *62*, 1252.
- (302) Kunitake, M.; Akiyoshi, K.; Kawatana, K.; Nakashima, N.; Manabe, O. *J. Electroanal. Chem.* **1990**, *293*, 277.
- (303) *Langmuir-Blodgett Films*; Roberts, G., Ed.; Plenum Press: New York, 1990.
- (304) Bilewicz, R.; Majda, M. *Langmuir* **1991**, *7*, 2794.
- (305) Bilewicz, R.; Majda, M. *J. Am. Chem. Soc.* **1991**, *113*, 5464.
- (306) Nelson, A. J. *J. Electroanal. Chem.* **1991**, *303*, 221.
- (307) Nelson, A. J. *J. Chem. Soc., Faraday Trans.* **1991**, *87*, 1851.
- (308) Okahata, Y.; Tsuruta, T.; Ijiro, K.; Ariga, K. *Langmuir* **1988**, *4*, 1373.
- (309) Sun, S.; Ho-Si, P.-H.; Harrison, D. J. *Langmuir* **1991**, *7*, 727.
- (310) Bourdillon, C.; Majda, M. *J. Am. Chem. Soc.* **1990**, *112*, 1795.
- (311) Parpaleix, T.; Laval, J. M.; Majda, M.; Bourdillon, C. *Anal. Chem.* **1992**, *64*, 641.

- (312) Ahlers, M.; Muller, W.; Reichert, A.; Ringsdorf, H.; Venzmer, J. *Angew. Chem. Int. Ed. Engl.* **1990**, *29*, 1269.
(313) Gronberg, L.; Slotte, J. P. *Biochemistry* **1990**, *29*, 3173.
(314) Pisarchick, M. L.; Thompson, N. L. *Biophys. J.* **1990**, *58*, 1235.
(315) Marcus, R. A.; Sutin, N. *Biochim. Biophys. Acta* **1985**, *811*, 265.
(316) Marcus, R. A. *J. Chem. Phys.* **1956**, *24*, 966.
(317) Marcus, R. A. *J. Chem. Phys.* **1965**, *43*, 679.
(318) Zusman, L. D. *Chem. Phys.* **1980**, *49*, 295.
(319) Weaver, M. J. *Chem. Revs.* **1992**, *92*, 463.
(320) Zhang, X.; Yang, H.; Bard, A. J. *J. Am. Chem. Soc.* **1987**, *109*, 1916.
(321) Zhang, H.; Murray, R. W. *J. Am. Chem. Soc.* **1991**, *113*, 5183.
(322) Zhang, H.; Murray, R. W. *J. Am. Chem. Soc.*, in press.
(323) Andrieux, C. P.; Saveant, J.-M. In *Molecular Design of Electrode Surfaces, Techniques of Chemistry*, Vol. 22; Murray, R. W., Ed.; John Wiley & Sons: New York, 1992; p 207.
(324) Majda, M. In *Molecular Design of Electrode Surfaces, Techniques of Chemistry*, Vol. 22; Murray, R. W., Ed.; John Wiley & Sons: New York, 1992; 159.
(325) Inzelt, G. In *Electroanalytical Chemistry*, Vol. 18; Bard, A. J., Ed.; Marcel Dekker: New York, 1993, in press.
(326) Blanch, D. N.; Saveant, J.-M. *J. Am. Chem. Soc.* **1992**, *114*, 3323.
(327) Fritsch-Faules, I.; Faulkner, L. R. *J. Electroanal. Chem.* **1989**, *263*, 237.
(328) Anson, F. C.; Blanch, D. N.; Saveant, J.-M.; Shu, C. F. *J. Am. Chem. Soc.* **1991**, *113*, 1922.
(329) Andrieux, C. P.; Saveant, J.-M. *J. Phys. Chem.* **1988**, *92*, 6761.
(330) Serra, A. M.; Mariani, R. D.; Abrufia, H. D. *J. Electrochem. Soc.* **1986**, *87*, 2226.
(331) Jernigan, J. C.; Surridge, N.; Avanut, M. E.; Silver, M.; Murray, R. W. *J. Phys. Chem.* **1989**, *93*, 4620.
(332) Dalton, E. F.; Surridge, N. A.; Jernigan, J. C.; Wilbourn, K. O.; Facci, J. S.; Murray, R. W. *Chem. Phys.* **1990**, *141*, 143.
(333) Surridge, N. A.; Zvanut, M. E.; Keene, F. R.; Sosnoff, C. S.; Silver, M.; Murray, R. W. *J. Phys. Chem.* **1992**, *96*, 962.
(334) Han, D.; Shimada, S.; Murray, R. W.; Silver, M. *Phys. Rev.* **1992**, *45*, 9436.
(335) Geng, L.; Ewing, A. G.; Hernigan, J. C.; Murray, R. W. *Anal. Chem.* **1986**, *58*, 852.
(336) McDevitt, J. T.; Ching, S.; Sullivan, M.; Murray, R. W. *J. Am. Chem. Soc.* **1989**, *111*, 4528.
(337) O'Connell, K. M.; Evans, D. H. *J. Am. Chem. Soc.* **1983**, *105*, 1473.
(338) Ching, S.; McDevitt, J. T.; Peck, S. R.; Murray, R. W. *J. Electrochem. Soc.* **1991**, *138*, 2308.
(339) *Polymer Electrolyte Reviews 1*; MacCallum, J. R.; Vincent, C. A., Eds.; Elsevier Appl. Sci.: London, 1987.
(340) Armand, M. B. *Annu. Rev. Mater. Sci.* **1986**, *16*, 245.
(341) Vincent, C. A. *Prog. Solid State Chem.* **1987**, *17*, 145.
(342) Ratner, M. A.; Shriver, D. F. *Chem. Rev.* **1988**, *88*, 109.
(343) Geng, L.; Reed, R. A.; Kim, M.-H.; Wooster, T.; Oliver, B. N.; Egekeze, J.; Kennedy, R.; Jorgenson, J. W.; Parcher, J. F.; Murray, R. W. *J. Am. Chem. Soc.* **1989**, *111*, 1614.
(344) Watanabe, M.; Longmire, M. L.; Murray, R. W. *J. Phys. Chem.* **1990**, *94*, 2614.
(345) Pinkerton, M.; LeMest, I.; Zhang, H.; Watanabe, M.; Murray, R. W. *J. Am. Chem. Soc.* **1990**, *112*, 3730.
(346) Bard, A. J.; Fan, F.-R. F. *Faraday Discuss.*, in press.